EFFECT OF HEPATOCYTE-SPECIFIC INACTIVATION OF DIVALENT METAL-ION TRANSPORTER-1 (DMT1) ON IRON HOMEOSTASIS AND CHARACTERIZATION OF ZIP8 AS A NOVEL IRON TRANSPORTER

By

CHIA-YU WANG

A DISSERTATION PRESENTED TO THE GRADUATE SCHOOL
OF THE UNIVERSITY OF FLORIDA IN PARTIAL FULFILLMENT
OF THE REQUIREMENTS FOR THE DEGREE OF
DOCTOR OF PHILOSOPHY

UNIVERSITY OF FLORIDA

2012

To my wonderful parents

ACKNOWLEDGMENTS

Completion of my dissertation could not have been possible without the guidance of my committee members, help from colleagues and friends, and the support of my family.

I would like to express my deepest gratitude to my major advisor Dr. Mitchell D. Knutson for the outstanding guidance and the patience shown throughout my doctoral studies. I thank my other committee members, Dr. Harry S. Sitren, Dr. James F. Collins and Dr. Jae-Sung Kim for their constructive comments and invaluable support over the years. I thank my first mentor, the late Dr. Hiromi Gunshin, who led me into the molecular iron field and ignited my passion for scientific research.

Hyeyoung Nam, Ningning Zhao, Supak Jenkitkasemwong, Wei Zhang, Lin Zhang, and Richard S. Coffey, who are my colleagues and friends. They always help me in various aspects in experiments as well as in life.

I sincerely thank my father, Wen-Ching Wang, and my mother, Mei-Chin Liao, for their love, understanding, support and encouragement.

TABLE OF CONTENTS

page

LIST OF TABLES

LIST OF FIGURES

LIST OF ABBREVIATIONS

CCS	Copper chaperone for superoxide dismutase
DCYTB	Duodenal cytochrome b
DMEM	Dulbecco's modified Eagle's medium
DMT1	Divalent metal-ion transporter-1
FBS	Fetal bovine serum
HH	Hereditary hemochromatosis
HIF	Hypoxia inducible factor
ICP-MS	Inductively coupled plasma mass spectrometry
IRE	Iron responsive element
IRP	Iron regulatory protein
TBI	Transferrin-bound iron
L-DOPA	3,4-dihydroxyphenylalanine
LPS	Lipopolysaccharide
NDFIP	Nedd4 family interacting protein
NTA	Nitrilotriacetic acid
NTBI	Non-transferrin-bound iron
PNGASE F	Peptide: N-Glycosidase F
SLC11A2	Solute carrier family 11, member 2
SLC46A1	Solute carrier family 46, member 1
TFR1	Transferrin receptor 1
TFR2	Transferrin receptor 2
TF-TFR	Transferrin-transferrin receptor
SRB1	Scavenger receptor class B type I
WT	wild-type

ZIP8	ZRT/IRT-like Protein 8
$ZnCl_2$	Zinc chloride

Abstract of Dissertation Presented to the Graduate School
of the University of Florida in Partial Fulfillment of the
Requirements for the Degree of Doctor of Philosophy

EFFECT OF HEPATOCYTE-SPECIFIC INACTIVATION OF DIVALENT METAL-ION TRANSPORTER-1 (DMT1) ON IRON HOMEOSTASIS AND CHARACTERIZATION OF ZIP8 AS A NOVEL IRON TRANSPORTER

By

Chia-Yu Wang

December 2012

Chair: Mitchell D. Knutson
Major: Nutritional Sciences

Divalent metal-ion transporter-1 (DMT1) is a transmembrane protein that is known to be essential for iron uptake by enterocytes and erythroid precursors. DMT1 is also present in the liver, where it is believed to play a role in hepatic iron uptake, either through transferrin-bound iron (TBI) or non-transferrin-bound iron (NTBI), which appears in the plasma during iron overload. I investigated the role of DMT1 in hepatic iron uptake by using DMT1 hepatocyte-specific knockout (*Dmt1*$^{liv/liv}$) mice and by crossing them with two mouse models of genetic iron overload. To directly access the role of DMT1 in NTBI and TBI uptake, I injected ^{59}Fe-labeled ferric citrate or ^{59}Fe-transferrin intravenously into *Dmt1*$^{liv/liv}$ and *Dmt1*$^{flox/flox}$ mice and measured hepatic ^{59}Fe uptake. I found that DMT1 is dispensable for hepatic iron accumulation or for NTBI uptake. Although TBI uptake was 40% lower in *Dmt1*$^{liv/liv}$ mice, the contribution to the overall iron economy of the liver is minor because hepatic iron levels were unaffected. Given that DMT1 is dispensable for hepatic iron homeostasis, other iron transport mechanisms must exist. One possibility is ZIP8 (ZRT/IRT-like Protein 8), a close homologue of ZIP14, a transmembrane protein that has recently been shown to transport iron. ZIP8

has been shown to transport zinc, cadmium, and manganese, but the capability of ZIP8 to mediate iron transport has not been reported. I tested the hypothesis that ZIP8 transports iron and investigated its regulation by iron and tissue distribution. I found that overexpression of ZIP8 in HEK 293T cells increased NTBI uptake by 200%. I also found that cell-surface ZIP8 is upregulated by iron loading in H4IIE cells, a rat hepatoma cell line, and that ZIP8 mediates NTBI uptake at both pH 7.5 and 6.5. By screening ZIP8 mRNA levels from 20 different human tissues, I found that ZIP8 was most abundantly expressed in the lung and placenta. Moreover, siRNA-mediated suppression of ZIP8 expression in BeWo cells, a placental cell line, decreased NTBI uptake by 37%. These data reveal ZIP8 as a novel iron transporter that may play a role in iron metabolism, possibly in hepatic iron uptake and/or in placental iron transport.

CHAPTER 1
LITERATURE REVIEW

In the first section of this chapter, I will provide a general overview of iron biological functions, body distribution, homeostasis, and overload disorders. In the second section, I will review DMT1, focusing on its function, regulation, and mutations that affect its function. In the last section, I will introduce ZIP8 and its possible relation to iron metabolism.

Biological Functions of Iron and Body Iron Distribution

Proteins containing iron can be divided into three groups: heme proteins, iron-sulfur proteins, and other iron-containing proteins. The most commonly recognized biological function of iron is as a constituent of the heme moiety in heme proteins. Heme proteins play diverse roles in the body, such as hemoglobin and myoglobin in oxygen transport (1-4), catalase and peroxidases in catalysis (5) and cytochromes in electron transfer (6). Iron-sulfur (Fe-S) cluster proteins usually contain equal numbers of iron and sulfide ions, 2Fe-2S or 4Fe-4S. These proteins function in electron transfer reactions, such as NADH dehydrogenase, succinate dehydrogenase and cytochrome *c* reductase in complex I, II and III of the mitochondrial electron transport chain, respectively (7). There are also non-redox enzymes containing Fe-S clusters, such as aconitase. Mitochondrial aconitase catalyzes the conversion of citrate to iso-citrate whereas cytosolic aconitase functions as an iron regulatory protein (IRP) when iron is scarce (8). Other iron-containing proteins do not have a heme moiety or an Fe-S cluster, such as hydroxylases. For example, prolyl hydroxylase catalyzes the synthesis of hydroxyproline in the production of collagen and tyrosine hydroxylase catalyzes the conversion of

tyrosine to 3,4-dihydroxyphenylalanine (L-DOPA), the rate-limiting step in the biosynthesis of catecholamines (9, 10).

An adult man contains approximately 3-5 gram of iron with 65% of total body iron in hemoglobin (11, 12) and 10-15% in myoglobin and other iron-containing enzymes (13). The remainder, approximately 20-25%, is stored in the liver, macrophages and bone marrow in the form of ferritin and/or hemosiderin (11, 14). Less than 1% of total body iron is in the circulation bound with transferrin (13). An adult female usually has 2-3 g of iron, but with low iron stores.

Iron Homeostasis

The ability of iron to donate and accept electrons contributes in large part to its involvement in enzymatic reactions and biological functions; however, too much iron can be toxic due to free radical generation through the Fenton reaction (15). Dietary iron absorption contributes 1-2 mg of iron daily on average and is needed to replace the same amount of iron lost through occult blood loss, desquamation of mucosal and skin cells, and menstruation in females (13, 14). Because there is no effective way of excreting excess iron (12), the regulation of iron absorption becomes critical in maintaining iron homeostasis in the body.

Intestinal Iron Absorption

Dietary sources of iron can be divided into two types, heme iron and nonheme iron. Heme iron only comes from animal sources, in which iron is locked within the porphyrin ring (16). Nonheme iron refers to all other forms of iron. For non-vegetarians, heme iron is only ~10% of total iron intake; however, it is more bioavailable and can contribute up to two thirds of absorbed iron (17).

Heme iron absorption

Dietary heme is absorbed intact by enterocytes and the iron is released from the heme moiety by heme oxygenase (18-20). The liberated iron enters a low-molecular-weight pool containing absorbed dietary nonheme iron before being transported out of the enterocyte through ferroportin, a transmembrane protein situated on the basolateral membrane (21, 22). Recently, the protein SLC46A1 (solute carrier family 46, member 1) was identified as a heme iron transporter at the apical membrane of enterocytes by using subtractive hybridization screening in hypotransferrinemic mice (23). However, it was later shown to be a folate transporter by using a database mining approach based on homology to a facilitative reduced folate carrier (24). Indeed, compared to heme with a transport affinity K_m of 125 μM at neutral pH, SLC46A1 has a much higher affinity for 5-methyltetrahydrofolate (K_m = 0.8 μM at pH 6.5). Moreover, a mutation in this gene results in syndromes of hereditary folate malabsorption (23, 24). Therefore, the mechanistic details of heme iron absorption remain to be elucidated.

Nonheme iron absorption

The molecular mechanisms of nonheme iron absorption have been intensively studied since 1997, when the transporter DMT1 was identified (25). The official gene symbol of DMT1 is *Slc11a2*, solute carrier family 11, member 2 (26). DMT1 is abundantly expressed in the proximal duodenum, where it serves as the major iron importer at the apical membrane of epithelial cells (25, 26). As the majority of dietary nonheme iron is in ferric (Fe^{3+}) state (17), a cell-surface ferrireductase (27, 28) or reducing agent such as ascorbic acid (29) is required to reduce dietary ferric iron to its ferrous (Fe^{2+}) form before it can be transported across the intestinal epithelium. Duodenal cytochrome b (Dcytb; *Cybrd1*) was recognized as the ferrireductase at the

apical membrane of enterocyte; however, the lack of an iron-deficient phenotype in *Cybrd1* knockout mice raises the question of its essentiality (30). It is possible that, unlike humans which depend on exogenous sources of vitamin C, mice can synthesize ascorbic acid (31) and the concentration of ascorbic acid in small intestine is high (~2 µmol /g tissue) (32, 33) and therefore, a ferrireductase is not required. After iron traverses the apical membrane of enterocytes through DMT1, it can be either stored as ferritin or exported across the basolateral membrane via ferroportin. Ferroportin (*Slc40a1*) is the sole known iron exporter and it is required for transporting iron from enterocytes to the circulation (22). After export from the enterocyte, the ferrous ion is oxidized to the ferric (Fe^{3+}) form by hephaestin, a copper-dependent ferroxidase, before it binds to transferrin (34).

Circulation and Storage of Iron

The majority of iron in plasma is bound to transferrin. Under normal conditions, about one-third of total transferrin is loaded with iron whereas NTBI is nearly undetectable. NTBI refers to iron that is not in heme, ferritin or bound with transferrin, but in a low-molecular-mass form and bound with small ligands, such as citrate and albumin (35, 36). In iron overload conditions, the amount of circulating iron can exceed the binding capacity of transferrin and plasma NTBI concentrations may increase up to 10 µM (37). Iron is stored inside the cell as ferritin or hemosiderin. Ferritin has two distinct subunits, H and L. Different proportions of H and L subunits assemble to form apoferritin, a 24-subunit hollow structure that can accommodate up to 4500 iron atoms (38). Ferritin is also present in the serum and is commonly used as an indicator of body iron stores. Serum ferritin is secreted by macrophages (39) and can increase to over 2500 ng/mL in β-thalassemia patients (40). Hemosiderin, a water-insoluble protein with

a high iron-to-protein ratio, is thought to be product of lysosomal degradation of ferritin and observed primarily in iron-loaded tissues (41, 42).

Hepcidin Regulates Iron Homeostasis

Hepcidin is a 25-amino acid peptide hormone secreted by hepatocytes. Hepcidin circulates in blood plasma and prevents iron efflux from enterocytes, hepatocytes, and macrophages, and therefore, lowers plasma iron concentrations (43, 44). Hepcidin regulates cellular iron efflux by binding to the iron exporter ferroportin and inducing its internalization and degradation (45). Hepcidin is regulated by a number of conditions including anemia, hypoxia, inflammation, and iron overload (46, 47).

Iron Overload Disorders

Iron overload is a serious consequence in patients with hereditary hemochromatosis and in patients with bone marrow defects who undergo blood transfusions. Early signs of iron overload are increased transferrin saturation and elevated concentrations of plasma iron and ferritin (48). Accumulation of iron can lead to irreversible tissue damage, fibrosis and organ failure due to the formation of damaging oxygen radicals catalyzed by free iron (13, 49). The main tissues affected are the liver, heart, and pancreas, resulting in increased risks of hepatocellular carcinoma, cirrhosis, cardiomyopathy, and diabetes (13, 50).

Primary Iron Overload

Primary iron overload or hereditary hemochromatosis (HH) is a genetic disorder that results from increased absorption of dietary iron. In HH, a homozygous substitution of tyrosine for cysteine at position 282 (C282Y) in the HFE protein is the most common mutation with a prevalence of about 1 in 200 to 400 individuals of Northern European descent (51-53). Another missense mutation found in *HFE* results in the substitution of

histidine with aspartate at position 63 (H63D). Although the most common *HFE* mutation in HH is C282Y, H63D substitution is the most common *HFE* mutation overall. The prevalence of H63D homozygotes or compound heterozygotes (C282Y/H63D) is about 1:50 (52, 54); however, this mutation has a much lower penetrance than C282Y mutation (55-57). Individuals with *HFE*-associated hemochromatosis usually present with clinical symptoms in the fourth or fifth decade of life.

Other mutations that contribute to hemochromatosis include those in genes encoding hemojuvelin (*HJV*), hepcidin (*HAMP*), transferrin receptor 2 (*TFR2*) and ferroportin (*SlC40A1*). Mutations in *HFE, TFR2, HJV*, and *HAMP*, result in dysregulation of hepcidin that leads to systemic iron overload (50). With these mutations, hepcidin levels are low due to a defect in *HAMP* itself or a regulator of hepcidin. *HJV* and *HAMP* mutations cause accelerated iron loading and early onset organ disease, usually before the age of 30 (58-60); therefore, it is also called juvenile hemochromatosis. Mutations in ferroprotin are inherited in an autosomal-dominant fashion. Some mutations, such as A77D and W158C, are either loss-of-function or result in impaired trafficking to the plasma membrane, and therefore, iron accumulates predominantly in reticuloendothelial cells (61, 62). With other mutations, such as N144H and H507R, ferroportin appears to lose its ability to interact with hepcidin, thereby mimicking hepcidin deficiency, and leading to hemochromatosis (62-64).

Secondary Iron Overload

Secondary iron overload results from blood transfusions, such as in the treatment β-thalassemia (65). Patients with β-thalassemia have a defect in β-globin synthesis, resulting in deficient hemoglobin synthesis and anemia (66). Severe forms usually arise from homozygosity or compound heterozygosity and affected patients require blood

transfusions to survive (66, 67). Blood transfusions increase body iron burden, leading to increased iron loading in tissues (68). As these patients are also anemic, they have increased iron absorption, which further contributes to iron loading (69, 70). Phlebotomy and chelation therapies have been used in patients with hereditary hemochromatosis (71). Patients with secondary iron overload are treated with chelation therapy to relieve iron overload caused by blood transfusions (72). However, both phlebotomy and chelation treatments have adverse side effects. Once the molecular mechanisms of iron uptake in tissues are further clarified, researchers will be able to target the responsible molecule(s) to develop new treatments that can help these patients.

Divalent Metal-ion Transporter-1

DMT1 was cloned from iron-deficient rat duodenum in 1997 and is the first mammalian iron transporter identified (25). Functional studies using *Xenopus* oocytes revealed that it transports not only iron, but also other divalent metals including Cd^{2+}, Co^{2+}, Mn^{2+} and Ni^{2+} (25, 73). *Dmt1* mRNA has four different isoforms differing in their 3' and 5' ends that are derived from alternative splicing and alternative promoters. Alternative splicing at the 3' end yields two variants – the IRE and non-IRE forms. The IRE form of *Dmt1* mRNA harbors an iron-responsive element (IRE) in its 3' untranslated region (UTR) whereas the non-IRE form does not (74). At the 5' end, the two variants (*Dmt1-1A* and *Dmt1-1B*) derive from alternative promoter usage resulting in different 5' exons (75). Regulation and expression of these four isoforms appears to be tissue specific (75).

DMT1 Mutations in Rodents and Humans

Rodents

Mutations in *Dmt1* have been identified in the microcytic anemia (*mk*) mouse and the Belgrade (*b*) rat. Both mutant animal models have severe hypochromic microcytic anemia due to a single nucleotide, glycine-to-arginine, substitution at amino acid codon 185 (G185R) of DMT1 that leads to impaired iron absorption and erythroid iron utilization (76, 77). Functional analyses in HEK293T (Human Embryonic Kidney) cells transfected with mutant constructs have established that the G185R mutation diminishes transport activity by altering the function of DMT1, rather than affecting levels of protein expression (78). Studies in *mk* mice further demonstrated that, although intestinal DMT1 expression was greatly induced, the mutation impaired its targeting to brush-border membrane thus affecting iron absorption (79).

Humans

Mutations in human *DMT1* have been reported in five unrelated cases. Most of *DMT1* mutations have been associated with hypochromic microcytic anemia and hepatic iron overload (80-83). The first case reported was a missense mutation, a G to C transition in exon 12 of the *DMT1* gene (1285 G>C), that resulted in two consequences: (i) 90% of the transcripts have exon 12 deleted due to impaired splicing and (ii) the remaining 10% contained exon 12, but had E399D substitution in the protein (84). Immunofluorescence analysis and functional analysis revealed that the E339D mutant did not affect its targeting, expression or transport activities (85, 86), although one study suggested it may partially decrease transport ability (87). On the other hand, the deletion of exon 12 impaired protein targeting to endosomes, decreased the

expression of mature, complex-glycosylated form of DMT1, and abolished its transport activities (86, 87).

Three cases of compound heterozygous mutations have been identified. The first case is a 3-bp deletion in intron 4 resulting in abnormal splicing and a C>T transition in exon 13 (1246 C>T) resulting in R416C substitution (81). The 3-bp deletion caused 30-35% of the transcripts to have exon 5 deleted. Immunoblotting demonstrated that DMT1 protein levels in peripheral blood mononuclear cells (PBMCs) were decreased by 40% (81). Functional analysis of the stably expressed mutant protein revealed that the R416C substitution impaired DMT1 protein processing and transport activity (88). Immunofluorescence analysis suggested that the R416C mutant was retained in the endoplasmic reticulum and barely localized in the recycling endosome, consistent with its low cell-surface expression (88). The second heterozygous compound mutation was a GTG deletion in exon 5 (c.428-30) resulting in the deletion of V114 and a G>T substitution in exon 8 resulting in Gly 212 to Val (G212V) substitution (82). The last case of compound heterozygous mutation was the previously described G212V substitution and a novel N491S mutation (83). These mutants have not been functionally characterized except for the N491S substitution. Sequencing of mRNA isolated from peripheral blood revealed that the N491S mutation resulted in different mRNA splicing that may contribute to aberrant cell trafficking and impaired transport activity (83).

The only homozygous case of human *DMT1* mutation was in exon 4 (311G>A) resulting in a G75R substitution. Similar to others, this patient had microcytic anemia,

moderate serum iron levels and elevated transferrin saturation; however, no sign of liver iron overload was observed at the age of 7 (89).

Function of DMT1 in Intestine and Erythroid Cells

Studies using *mk* mice and the Belgrade rat have amply documented that erythroid precursors acquire iron through the transferrin-transferrin receptor (Tf-TfR) pathway, in which TBI enters developing red blood cells through receptor-mediated endocytosis of transferrin (90-93) and DMT1 transports iron out of the endosome and into the cytoplasm (77, 94) (Figure 1-1). Prior to transport by DMT1 in the endosome, Fe^{3+} is reduced to Fe^{2+} by six-transmembrane epithelial antigen of the prostate 3 (*Steap3*) (95). It was also shown that intestinal iron absorption in *mk* mice and *b* rat was impaired (96, 97). Studies in *Dmt1* knockout ($Dmt1^{-/-}$) mice have confirmed that DMT1 plays an essential role in iron acquisition by erythroid precursors and in intestinal iron absorption by the enterocyte (26).

Regulation of DMT1

Intestine

Anemia and erythropoiesis. DMT1 expression in the small intestine is responsive to both systemic and local signals of iron status. Iron deficiency anemia (25, 98, 99), and other conditions driving erythropoiesis, such as erythropoietin injected into rats (100) and phlebotomy in the treatment of HH patients (101), result in increased DMT1 expression at the mRNA and protein levels. Anemia caused by genetic mutations in mice, such as in *mk* and $Trf^{hpx/hpx}$ mice, also results in elevated DMT1 protein levels in the intestine. In *mk* mice, the G185R mutation causes improper targeting of the protein in the apical membrane (79, 102). Mice with a mutation in hephaestin (*Heph*) are anemic due to impaired iron transport out of enterocyte, but DMT1 protein expression is

not upregulated because of iron retention in enterocyte, suggesting local signals can modulate DMT1 expression despite the need for erythropoiesis (103).

Hepcidin and its modulators. Hepcidin, the hormone that plays an important role in regulating iron homeostasis (43) may also modulate DMT1 expression. In hepcidin-deficient (*Usf2*$^{-/-}$) mice, in spite of systemic iron overload (104), DMT1 protein expression was induced in the intestine, probably because upregulation of ferroportin resulted in low iron levels in the enterocyte (105). Similarly, in human intestinal Caco-2 cells (epithelial colorectal adenocarcinoma), hepcidin treatment significantly decreased DMT1 protein expression (106), supporting the concept that DMT1 expression is regulated by local signals of iron status.

Modulators that control hepcidin expression (i.e. HFE, TfR2, SMAD4), also regulate DMT1 expression. Studies in *Hfe*, *Tfr2* knockout as well as *Smad4* liver-specific knockout mice showed increase DMT1 expression in the intestine (107-109), possibly through downregulation of hepcidin expression (108-112). Consistent with this finding, duodenal DMT1 expression is upregulated in patients with both *HFE*-associated and non-*HFE*-associated hemochromatosis (113, 114). However, a study in HH patients with the *HFE* mutation showed increased intestinal *Dmt1* mRNA expression as well as stronger DMT1 staining in the apical membrane of duodenal tissue, but only when patients were treated by phlebotomy (101).

Iron Regulatory Proteins (IRPs). It is well established that when iron is scarce, IRPs bind to the IRE in the 3'UTR of transferrin receptor 1 (TfR1) to stabilize the mRNA transcript resulting in increased TfR1 protein translation and cellular iron acquisition (115-117). *Dmt1* mRNA isoforms also contain an IRE in the 3'UTR and intestinal DMT1

is responsive to iron deficiency (25, 74, 75, 118). A recent study by Galy *et al*.(119), investigated the role of IRPs *in vivo* by deleting IRPs specifically in the intestine. They found that inactivation of intestinal IRPs reduced DMT1 protein levels and resulted in abnormal duodenum development, nutrient malabsorption, growth defects, and lethality by 4 weeks of age (119).

Hypoxia Inducible Factors (HIFs). HIFs are transcription factors that are stabilized by hypoxia. They induce the expression of several genes involved in cell survival during low oxygen conditions (120). Studies of intestine-specific *Hif1α* and *Hif2α* knockout mice suggest that HIF2α induces DMT1 expression by directly interacting with the *Dmt1 1A* promoter (121).

Ferritin H. Ferritin H (*Fth*) is a subunit of ferritin that has ferroxidase activity. It is required for ferritin formation and was recently shown to regulate iron efflux from the enterocyte (122). Studies of intestine-specific *Fth* knockout mice showed increased hepcidin levels in response to systemic iron overload, and therefore *Dmt1* expression was decreased. Unexpectedly, intestinal ferroprotin levels were greatly induced and the mice displayed increased iron absorption, resulting in greater hepatic iron loading (122).

Liver

The literature regarding hepatic DMT1 and its regulation is very limited and inconclusive. DMT1 staining in rat liver was reported stronger in iron-loaded animals but diminished in the iron-deficient group, suggesting that hepatic DMT1 is regulated by iron (123). However, *Dmt1* mRNA expression was reported increased in iron-deficient liver in mice (124). Other conflicting observations have been reported in studies of the *Hfe* knockout ($Hfe^{-/-}$) mice, a mouse model of hereditary hemochromatosis. A microarray study examining changes in duodenal and hepatic gene expression in $Hfe^{-/-}$ as well as

wild-type (WT) mice that were challenged with iron dextran injections reported that hepatic *Dmt1* expression was unaffected by primary and secondary iron overload conditions (125). However, studies of primary hepatocytes isolated from *Hfe*$^{-/-}$ mice found higher *Dmt1* expression at the mRNA and protein levels (126).

Post-transcriptional regulation

More recently, DMT1 was reported to interact with the Nedd4 family interacting proteins (Ndfips), which recruits E3 ligases to promote ubiquitination and degradation of target proteins (127, 128). Overexpression of Ndfip1 and Ndfip2 in CHO (Chinese hamster ovary) cells inhibited DMT1 transport activity by ~35% (127). Studies of Ndfip1 knockout (*Ndfip*$^{-/-}$) mice fed with iron-deficient diet showed stronger duodenal DMT1 staining and increased transport activities (129). When *Ndfip*$^{-/-}$ mice were fed a standard diet, hepatic DMT1 protein levels were upregulated and primary hepatocytes isolated from *Ndfip*$^{-/-}$ mice showed a ~70% increase in transport activity (127). Perl's staining showed iron deposition in the periportal region of *Ndfip*$^{-/-}$ livers, when compared with WT littermates (127).

ZIP8, ZIP14 and the Possible Relation to Iron Homeostasis

A second research direction that I pursued involved studying the metal-ion transporter ZIP8. The name of the ZIP superfamily stands for **Z**rt- (zinc regulated transporter-), **I**rt-like (iron regulated transporter-like) **p**roteins. The ZIP superfamily is an important group of metal-ion transporters that import substrates across cellular membranes into the cytoplasm (131). Of the fourteen ZIP proteins encoded by human and mouse genomes, ZIP8 and ZIP14 are the most closely related: they are similar in

Reprinted with permission from 130. Jenkitkasemwong S, Wang CY, Mackenzie B, Knutson MD. Physiologic implications of metal-ion transport by ZIP14 and ZIP8. Biometals 2012.

length (462 vs. 489 amino acids); have ~50% amino acids identical; and each contains *N*-linked glycosylation sites in the N-terminal region (Figure 1-2). The similarity between the two proteins is notably evident in the putative transmembrane domains. The highly conserved transmembrane domains IV and V, with their metal-binding histidine and glutamic residues, have been proposed to comprise part of an ion channel (132).

ZIP14 and Iron Homeostasis

The ability of ZIP14 to transport zinc was established by transfection of ZIP14 cDNA in CHO and K562 (human erythroleukemia) cells, which resulted in accumulation of intracellular zinc (133, 134). Subsequently, it was found that overexpression of ZIP14 in HEK293H and Sf9 insect cells not only increased intracellular accumulation of zinc, but also NTBI, suggesting a role for ZIP14 in iron uptake (135). Moreover, the NTBI uptake activities decreased when *Zip14* mRNA was suppressed by siRNA in AML12 mouse hepatocyte cells (135), suggesting that ZIP14 plays a role in mediating hepatic iron uptake. This finding was of particular importance because only one other mammalian iron import protein, DMT1, was known. Similar to DMT1 being a broad-scope metal-ion transporter, ZIP14 transports not only zinc and iron, but also other divalent metals such as Cd^{2+} and Mn^{2+} in the *Xenopus* laevis oocyte heterologous expression system (136). Functional studies in both *Zip14* RNA-injected oocytes and HEK 293T cells expressing ZIP14 suggested that ZIP14-mediated iron transport is at both pH 7.5 and 6.5, but not at pH 5.5 (136, 137), in contrast to DMT1 with optimal function at pH 5.5 (25). Consistent with the finding that ZIP14 functions at pH 6.5, transfection of ZIP14 cDNA into HEK 293T cells promoted iron assimilation from transferrin (137), further supporting the role of ZIP14 in hepatic iron uptake.

Studies examining the tissue distribution of ZIP14 showed that it is most abundant in the liver, pancreas and heart (130), whereas DMT1 is abundantly expressed in kidney, brain and thymus (25). Comparing the transcript abundance of DMT1 and ZIP14 by measuring copy number in HepG2 (human hepatocellular carcinoma) cells, it was shown that ZIP14 abundance is 10 times higher than that of DMT1 (137). The difference in pH dependence and tissue distribution of DMT1 and ZIP14 suggest they may function in different tissues and/or different subcellular compartments.

Metal Transport Capability of ZIP8

ZIP8 was first identified from monocytes that were induced during innate immune activation and overexpression of ZIP8 in CHO cells increased intracellular zinc accumulation (138). Subsequently, overexpression of ZIP8 in mouse fetal fibroblasts stimulated the accumulation of cadmium and manganese (139, 140) suggesting ZIP8 may be also a broad-scope metal-ion transporter.

Regulation of ZIP8

A previous study examined the expression of all ZIP proteins in rat liver and found that *Zip8* mRNA expression was unaffected by iron deficiency or iron overload (141). Interestingly, in a microarray analysis of iron-deficient rat duodenum, *Zip8* was found to be down-regulated by iron deficiency (142). Inflammation is known to affect iron and zinc metabolism. Studies showed that ZIP8 mRNA expression was down-regulated in the liver of mice given lipopolysaccharide (LPS) (143) but unaffected in pulmonary artery endothelial cells (144). Other studies reported that *Zip8* mRNA was upregulated by LPS and TNFα in human monocytes (138) and by the activation of human T cells (145).

Tissue and Subcellular Distribution of ZIP8

The majority of studies examining tissue distribution of ZIP8 reported that *Zip8* is most abundantly expressed in lung, followed by testis, kidney and liver (139, 146, 147), however; there were only 6 tissues examined in these studies. In a study where 16 tissues were compared, *ZIP8* is most abundantly expressed in pancreas followed by placenta, lung, and liver (138). A number of studies investigated cellular localization of ZIP8 by overexpressing epitope-tagged ZIP8 in cell lines and detected it localized to the plasma membrane, consistent with its proposed role of transporting metals from the extracellular space into cytoplasm (139, 140, 148, 149). In addition to the plasma membrane, ZIP8 has also been detected in the cytosol (148), lysosomes (145), and mitochondria (148), although the significance remains unclear.

ZIP8 and Diseases

A single nucleotide polymorphism (SNP) in the *ZIP8* gene was reported to be associated with body mass index/obesity (150), the risk of coronary artery disease (151), and schizophrenia (152). The SNP rs13107325 at the *ZIP8* locus locates in exon 8 and results in A391T substitution that is associated with lower circulating levels of HDL cholesterol (151). The authors concluded that ZIP8 may be associated with HDL cholesterol through inflammation. With respect to schizophrenia, the SNP at *ZIP8* is thought to affect Zn/Mg homeostasis in the brain, possibly by disrupting the blood-brain barrier which results in high metal concentrations loading to neurotoxicity (152).

Consistent with ZIP8 being regulated by inflammation, it has been associated with human immunodeficiency virus (HIV) infection (153) and sepsis (154). *ZIP8* mRNA expression as well as intracellular zinc levels were found to be increased in monocytes from HIV-infected subjects (153) . Studies of zinc chelator TPEN-treated monocytes

revealed that high zinc level retained the resistance of apoptosis, suggesting that ZIP8 contributes to the survival of monocytes from HIV-infected subjects therefore affecting disease activity (153). With respect to sepsis, *ZIP8* mRNA was also found to increase in monocytes from septic subjects while the levels of plasma zinc were decreased, which correlated with increased severity of the disease (154).

In summary, the research described herein tested the hypothesis that DMT1 plays a role in hepatic iron uptake and accumulation. Studies were also undertaken to characterize another mammalian iron import protein, ZIP8, as a first step to investigate novel iron transport mechanisms.

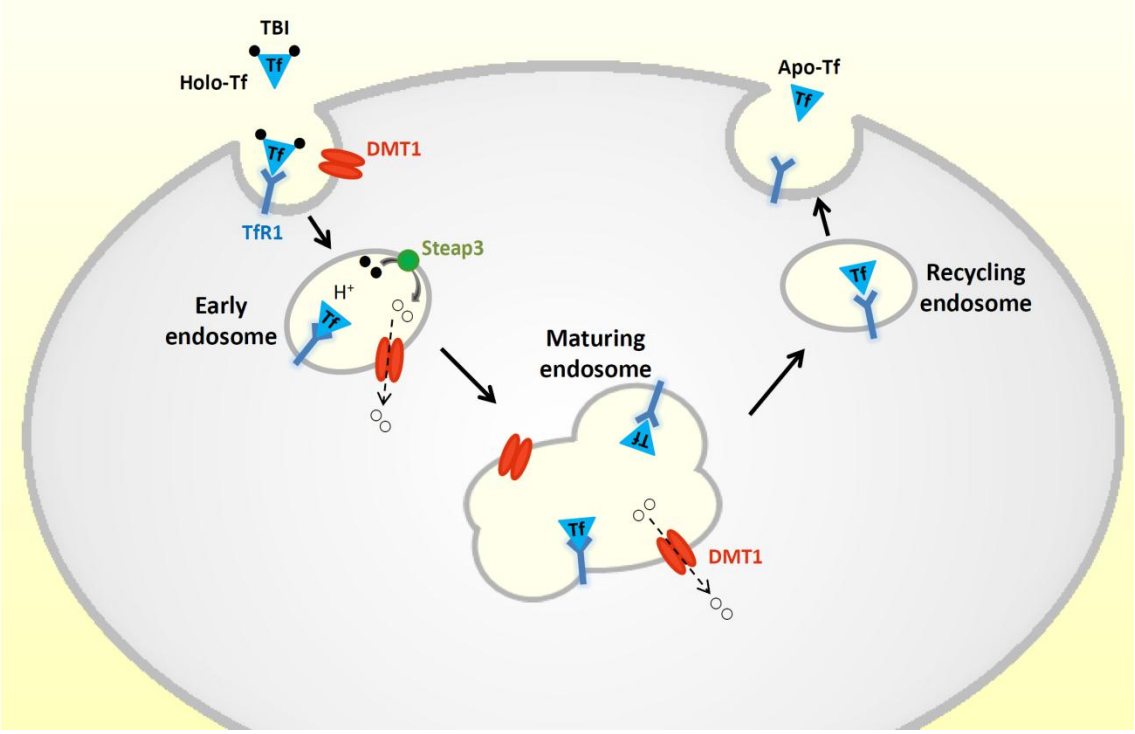

Figure 1-1. Model of DMT1 function in iron acquisition by erythroid precursors. The binding of holo-transferrin (Holo-Tf) and TfR1 induces endocytosis of the Tf-TfR1 complex. In the early endosome, acidification causes Tf to release ferric ion (Fe^{3+}), which is reduced to Fe^{2+} by Steap3 prior to transport into cytosol via DMT1. The Tf-TfR1complex recycles to the plasma membrane where apo-Tf dissociates from TfR1.

A

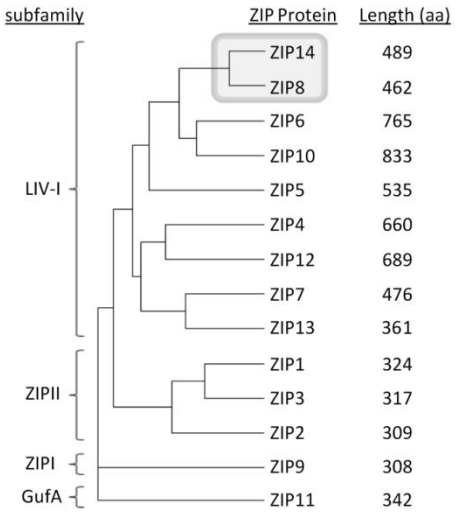

B

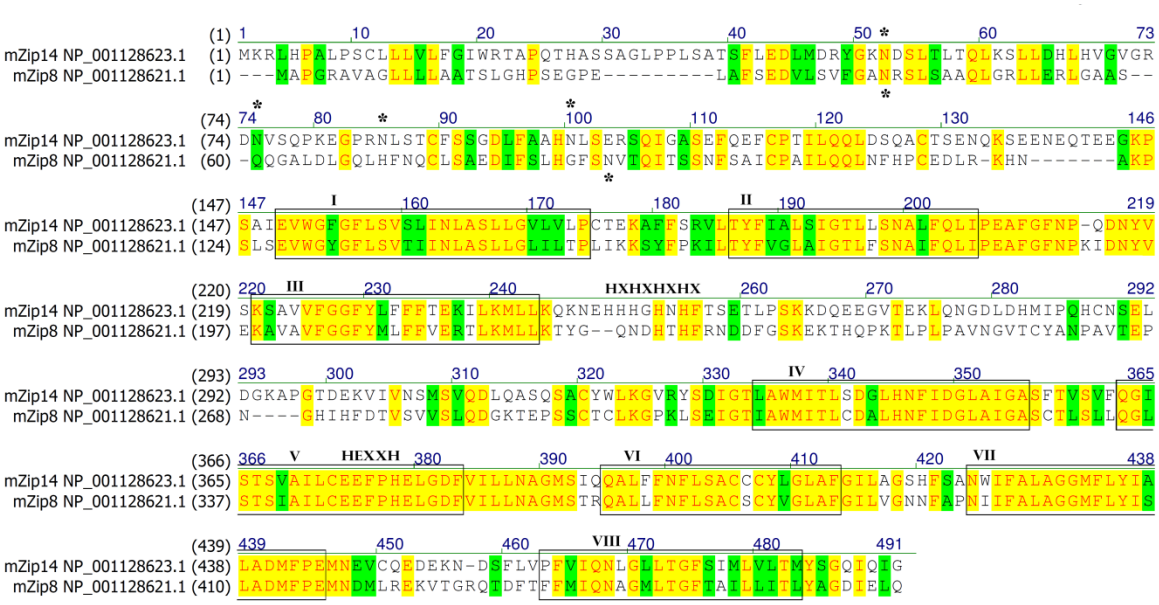

Figure 1-2. Similarity of ZIP14 and ZIP8 proteins. A) Simplified dendrogram showing relationships of the ZIP family proteins. B) Amino acid sequences for mZIP14 (NP_001128623.1) and mZIP8 (NP_001128621.1) were obtained from GenBank and aligned by using Vector NTI. Yellow shading indicates identical amino acids and green shading indicates conservative substitutions. Putative transmembrane (TM) domains, indicated by Roman numerals, were predicted by using MEMSAT-SVM. The histidine-rich repeat region (HXHXHXHX) between TM domains III and IV, the metalloprotease motif (HEXXH) in TM domains V, and the *N*-linked glycosylation sites are also indicated.

CHAPTER 2
MATERIALS AND METHODS

Animal Care and Genotyping

All animal protocols were approved by the Institutional Animal Care and Use Committee at the University of Florida. *Hfe*$^{-/-}$ (155), *Dmt1*$^{flox/flox}$ and *Dmt1*$^{liv/liv}$ (26) mice were on the 129S6/SvEvTac background. Hypotransferrinemic (*Trf*$^{hpx/hpx}$) mice were on BALB/cJ background (156). All mice were weaned at three weeks of age, maintained on a standard diet containing 240 ppm iron (Teklad 7912, Harlan Laboratories) and housed in a 12-h light-dark cycle. Mice were genotyped at weaning by extracting genomic DNA from snipped tail samples (DNeasy Blood & Tissue kit; Qiagen) and subjecting it to PCR analysis. To identify *Dmt1*$^{flox/flox}$ mice, I used primers F1: 5'-ATGGGCGAGTTAGAGGCTTT-3' and R1: 5'-CCTGCATGTCAGAACCAATG-3' (26). Cre-specific primers (F: 5'-TTACCGGTCGATGCAACGAGT-3'; R: 5'-TTCCATGAGTGAACGAACCTGG-3') were used to detect integration of the *Cre* gene into the mouse genome, and to identify *Dmt1*$^{liv/liv}$ mice. Primers F1 and R2: 5'-TTCTCTTGGGACAATCTGGG-3' (26) were used to confirm Cre-mediated excision in the liver. *Trf*$^{hpx/hpx}$ mice were identified at birth by their pallor and small size, and for survival, were injected intraperitoneally with human apo-transferrin (EMD Chemicals), 0.1 mL of a 6 mg/mL solution at 4 days of age, 0.2 mL in the second week and 0.3 mL weekly until 14 weeks of age. *Dmt1*$^{flox/flox}$ and *Dmt1*$^{liv/liv}$ mice were crossed with *Hfe*$^{-/-}$ and *Trf*$^{hpx/hpx}$ mice to produce double-mutant strains along with single-mutant strains on the same genetic background.

Measurement of mRNA Levels

Total RNA was extracted from flash-frozen tissue by using RNAzol® RT solution (Molecular Research Center, Inc.). Transcript abundance of *Dmt1* (all isoforms) was determined by using quantitative RT-PCR with forward primer 5'-TCCTCATCACCATCGCAGACACTT -3', located within exon 7, and reverse primer 5'-TCCAAACGTGAGGGCCATGATAGT -3', located within exon 8 of the murine *Dmt1* gene (75). Ribosomal protein L13a (*Rpl13a*) was quantified as an internal control by using forward primer 5'- GCAAGTTCACAGAGGTCCTCAA -3' and reverse primer 5'-GGCATGAGGCAAACAGTCTTTA -3'.

Transcript copy numbers of *ZIP8*, *ZIP14* and *DMT1* mRNA in human RNA (Human Total RNA Master Panel II, Clontech) were determined by using quantitative RT-PCR and standard curves generated from plasmids pCMV-Sport6-human ZIP8 (BC012125; Open Biosystems), pCMV-XL4-human ZIP14 (BC015770; Open Biosystems) and pBluescriptR-human DMT1 (BC100014; Open Biosystems).

Crude Membrane and Tissue Homogenate Preparation

Liver crude membrane fraction was used to measure DMT1, TfR1 and TfR2. To isolate membranes, liver samples were homogenized by a Dounce homogenizer in ice-cold HEM buffer (20 mM HEPES, 1 mM EDTA, 200 mM mannitol, pH 7.4) containing 1X complete mini protease inhibitor cocktail (Roche). The homogenate was centrifuged at 10,000 x *g* for 10 min at 4 ºC to pellet insoluble cell debris. The supernatant was centrifuged at 100,000 x *g* for 30 min at 4 ºC and the membrane pellet was then resuspended in HEM buffer. To measure ZIP14, tissues were homogenized in ice-cold RIPA lysis buffer (50 mM Tris pH 7.4, 150 mM NaCl, 1% IGEPAL CA-630 (Sigma-Aldrich), 0.5% Na deoxycholate, 0.1% SDS) containing protease inhibitors.

Homogenates were centrifuged at 10,000 x *g* for 10 min at 4 ºC to pellet and remove insoluble cell debris. Total protein concentration was determined colorimetrically by using the *RC DC* protein assay (Bio-Rad).

Western Blot Analysis

Proteins were mixed with Laemmli buffer and eletrophoretically separated on a 7.5% SDS-polyacrylamide gel. Before loading into the gel, samples analyzed for TfR1 and TfR2 were heated at 95 ºC for 5 min. For DMT1 and ZIP8, samples were incubated at 37 ºC for 30 min. For ZIP14, samples were not heated prior to electrophoresis. The separated proteins were transferred to nitrocellulose membranes (Schleicher and Schuell) and incubated for 1 h in blocking buffer (5% nonfat dry milk in Tris-buffered saline with 0.1 % Tween 20, TBST). Blots were then incubated overnight at 4 ºC in blocking buffer containing anti-DMT1 antiserum (1:2000; courtesy of Dr. Philippe Gros, McGill University, Montreal, Canada), mouse anti-TfR1 (1:4000, Invitrogen), rabbit anti-TfR2 (1:2500, Santa Cruz), 1 µg/mL affinity-purified rabbit anti-ZIP14, or 2 µg/mL affinity-purified rabbit anti-ZIP8. After washing blots in TBST, blots were incubated 40 min with species-specific horseradish peroxidase-conjugated secondary antibodies. Immunoreactivity was visualized by using enhanced chemiluminescence (SuperSignal West Pico, Pierce) and X-ray film or the FluorChem E digital darkroom (ProteinSimple). For loading control, blots were stripped and reprobed with mouse anti- Na^+/K^+ ATPase (1:10,000, Santa Cruz), rabbit anti-scavenger receptor class B type I, SR-B1, (1:5000; Novus Biologicals), rabbit anti-copper chaperone for superoxide dismutase, CCS (1:5000; Santa Cruz Biotechnology) or mouse anti-tubulin (1:10,000; Sigma-Aldrich) and processed as described above.

Iron Status Parameters, Liver Mineral Concentrations and Histological Analysis

Hemoglobin was measured in heparinized blood by using a HemoCue 201+ hemoglobin analyzer (HemoCue). Plasma was obtained by centrifugation of heparinized blood at 2,000 x *g* at 4 ºC for 10 min. Plasma iron and total iron binding capacity (TIBC) were determined as described previously (157). Transferrin saturation was calculated as plasma iron/TIBC x100. Tissue nonheme iron concentrations were determined by using the method of Torrance and Bothwell (1968). Briefly, 0.05 g of tissue was incubated in 1 mL acid solution (3M HCl and 10% trichloroacetic acid) at 65˚C for at least 20 h. Chromogen reagent (0.1% bathophenanthroline sulfphonate and 1% thioglycolic acid) was added and tissue nonheme iron was determined colorimetrically at absorbance 535 nm. Hepatic concentrations of total iron (nonheme and heme), zinc, copper, manganese, and cobalt were measured by using inductively coupled plasma mass spectrometry (ICP-MS). For histological analysis, livers fixed in 10% neutral buffered formalin for 20 h were subjected to routine histologic processing. Sections were deparaffinized and stained for ferric iron deposits by using Perls' Prussian blue stain.

Measurement of TBI and NTBI Uptake

For TBI uptake, *Dmt1*$^{liv/liv}$ and *Dmt1*$^{flox/flox}$ mice were injected with 150 µg of ^{59}Fe-transferrin (2 µCi) intravenously. For NTBI uptake, mice were injected with 70 µg ferric citrate to transiently saturate plasma transferrin. After 10 min, ^{59}Fe-labeled ferric citrate (2 µCi) was administered intravenously. Mice were sacrificed 2 h after ^{59}Fe was administered and whole-body counts per minute (cpm) were measured by using Perkin Elmer Wizard gamma counter. Tissues were harvested and cpm was determined for each organ to calculate percentage TBI or NTBI uptake.

Cell Culture

HEK 293T (human embryonic kidney) and H4IIE (rat hepatoma) cells were maintained in Dulbecco's modified Eagle's medium (DMEM; Mediatech) and BeWo (human choriocarcinoma) cells were maintained in F-12K medium with L-glutamine (ATCC). All media were supplemented with 10% (v/v) fetal bovine serum (FBS; Atlanta Biologicals), 100 units/mL penicillin and 100 µg/mL streptomycin. Cells were maintained at 37 ºC in 5% CO_2.

Immunoprecipitation

H4IIE total cell lysates were pre-cleared with 50 µL EZview Red Protein A Affinity Gel (Sigma-Aldrich) for 1 h at 4 ºC to minimize non-specific binding. ZIP8 or non-relevant antibody (CCS) was gently mixed with the affinity gel for 3 h at 4 ºC. Lysates were then added into bead-antibody mixtures and incubated at 4 ºC overnight. To elute samples, 2X Laemmli buffer and 5% 2-mercaptoethanol were added and samples were boiled for 10 min.

Measurement of Iron and Zinc Uptake

HEK 293T cells were transiently transfected with rZIP8 (GenBank accession number BC089844) or empty vector pExpress-1(Open Biosystems) for 48 h (Fugene HD, Roche). Prior to uptake, cells were washed twice with serum-free medium (SFM) and incubated for 1 h in SFM containing 2% BSA to deplete cells of transferrin and to block nonspecific binding at 37 ºC in 5% CO_2. For uptake, cells were incubated with 2 µM ^{59}Fe-ferric citrate in SFM in the presence of 1 mM ascorbate for 2 h at 37 ºC with or without a 10-fold molar excess of zinc, followed by three washes with an iron chelator solution (1 mM bathophenanthroline sulfonate and 1 mM diethylenetriaminepentaacetic acid) to remove surface-bound iron. Cells were lysed in buffer containing 0.2 N NaOH

and 0.2% SDS. Radioactivity was determined by gamma counting and protein concentration was determined colorimetrically by using the *RC DC* protein assay (Bio-Rad).

Measurement of pH-Dependence of ZIP8-mediated Iron Transport Activity

The pH-dependent iron transport activity was determined as previously described (137). Briefly, the uptake buffer (130 mM NaCl, 10 mM KCl, 1 mM $CaCl_2$ and 1 mM $MgSO_4$) was adjusted to pH 7.5, 6.5, and 5.5 by using 20 mM Hepes or MES buffers (158). Cells transiently transfected for 48 h with mZIP8 (GenBank accession number BC006731) or empty vector pCMVSport6 were washed twice with SFM and incubated for 1 h in SFM containing 2% BSA at 37 ºC in 5% CO_2. For uptake, cells were incubated with 2 µM ^{59}Fe-ferric citrate in uptake buffer in the presence of 1 mM ascorbic acid at 37 ºC for 60 min.

Iron Loading and Cell-Surface Biotinylation

To load cells with iron, H4IIE cells were treated with 100 or 250 µM ferric nitrilotriacetic acid (NTA) for 72 h. Cell-surface proteins were isolated by using the Pierce Cell Surface Protein Isolation kit according to the manufacturer's instructions (Thermo Scientific). Briefly, H4IIE cells were exposed to EZ-Link Sulfo-NHS-SS-Biotin to biotinylate cell-surface proteins, which were subsequently affinity purified by using NeutrAvidin Agarose resin. Bound proteins were released by incubating with SDS-PAGE buffer containing 50 mM DTT.

Assessment of *N*-linked Glycosylation

To inhibit *N*-glycosylation of endogenous ZIP8, H4IIE cells were incubated with 2 µg/mL tunicamycin for 48 h. To remove *N*-linked glycans, samples were incubated with denaturing buffer containing 1% 2-mercaptoethanol and 0.5% SDS for 30 min at 37 ºC

and then digested with Peptide: *N*-Glycosidase F (PNGase F) (50,000 unit/mL of sample volume or 50 units/ µg protein; New England Biolabs) for 2 h at 37 ºC.

Suppression of ZIP8 Expression in BeWo Cells

BeWo cells were reverse transfected with 50 nM siRNA targeting *ZIP8* mRNA (FlexiTube siRNA, Qiagen) or AllStars Negative Control siRNA (Qiagen) by using Lipofectamine RNAiMax (Invitrogen). After 72 h, cells were lysed in RIPA buffer and analyzed by Western blotting. For primary antibody, rabbit anti-human SLC39A8, Prestige antibody (Sigma-Aldrich) was used at 1:5000.

Statistical Analysis

Data are presented as means ± standard error (SE). Group means were compared by Student's unpaired *t* test. When more than two group means were compared, data were analyzed by one-way ANOVA with Tukey's post-hoc test. A *P*-value < 0.05 was considered statistically significant. Analyses were performed by using Prism (version 5; GraphPad) software.

CHAPTER 3
EFFECT OF HEPATOCYTE-SPECIFIC INACTIVATION OF DIVALENT METAL-ION TRANSPORTER-1 (DMT1) ON IRON HOMEOSTASIS

Introduction

Iron overload is a serious consequence in patients with hereditary hemochromatosis and in patients with bone marrow defects who undergo blood transfusions. Accumulation of iron can lead to irreversible tissue damage, fibrosis and organ failure due to the formation of damaging oxygen radicals catalyzed by free iron (13, 49). As the main tissues affected are the liver, heart, and pancreas, tissue iron overload is associated with various disorders, including liver cirrhosis, cardiomyopathy, and diabetes (13, 50). There are two forms of iron in blood plasma: TBI and NTBI. Under normal conditions, >95% of plasma iron is bound to transferrin. However, during iron overload, the amount of iron in plasma can exceed the carrying capacity of transferrin, giving rise to NTBI, which is bound to small ligands, mainly by citrate (126, 159, 160). In iron overload, both transferrin saturation and NTBI levels are high. After iron is absorbed in the intestine, it is transported to the liver, the main excess iron storage organ. However, the mechanisms involved in hepatic iron uptake and accumulation are not fully understood.

DMT1 is the first mammalian iron transporter identified. It is a proton-coupled metal-ion transporter that transports not only iron, but also other cation metals, such as Cd^{2+}, Co^{2+}, Mn^{2+} and Ni^{2+} (25, 73). Studies have conclusively demonstrated that DMT1 is the major iron transporter in the apical membrane of epithelial cells and is essential

---

Reprinted with permission from Wang CY, Knutson MD. Hepatocyte divalent metal-ion transporter-1 is dispensable for hepatic iron accumulation and non-transferrin-bound iron uptake in mice. Submitted to Hepatology.

for iron utilization in erythroid precursors, where TBI enters the cell through receptor-mediated endocytosis of transferrin and DMT1 transports iron out of the endosome and into the cytoplasm (26, 77). As DMT1 is present in the liver (25), it is possible that hepatocyte DMT1 releases iron from endosomes in the transferrin cycle. Hepatocytes can also acquire iron from NTBI (126). A previous study showed that overexpression of DMT1-GFP in human hepatoma (HLF) cells increased ferrous iron uptake, indicating that DMT1 in hepatocytes may play a role in NTBI uptake (161). The role of DMT1 in hepatocytes has also been implicated *in vivo*. Studies have shown that DMT1 staining in rat liver was stronger in iron-loaded animals and diminished in an iron-deficient group (123) and that NTBI uptake, along with DMT1 protein levels, was increased in primary hepatocytes from *Hfe*$^{-/-}$ mice (126). These data suggest that DMT1 may play a role in hepatic iron uptake. In contrast, elevated hepatic iron levels was observed in *Dmt1*$^{-/-}$ neonates and in Belgrade rats consuming a high-iron diet, suggesting that DMT1 is dispensable for iron uptake by the liver (30, 162). However, this observation was confounded by the fact that *Dmt1*$^{-/-}$ mice had severe anemia and prominent extramedullary erythropoiesis (26). Belgrade rats were also anemic and had elevated levels of serum iron and transferrin saturation when fed a high-iron diet (162). When iron dextran was injected into *Dmt1*$^{-/-}$ neonates, iron accumulated in hepatocytes as well as macrophages (26). Although these data indicate that at least one non-DMT1 involved pathway exists in hepatocytes, it is unclear how relevant these data are to usual pathways of hepatic iron uptake and accumulation. Nonetheless, it has been widely accepted that DMT1 plays a role in NTBI uptake in the liver (83, 129, 163-170). In this chapter, I used a conditional knockout mouse model in which DMT1 was inactivated

specifically in hepatocytes (*Dmt1*$^{liv/liv}$). I also crossed *Dmt1*$^{liv/liv}$ with two genetically modified iron overload mouse models, *Hfe*$^{-/-}$ and *Trf*$^{hpx/hpx}$ mice, to evaluate if DMT1 plays a role in liver iron accumulation during iron overload conditions. *Hfe*$^{-/-}$ mice are an animal model of hereditary hemochromatosis (171). In *Hfe*$^{-/-}$ mice, iron absorption is increased due to abnormally low levels of hepcidin, the iron-regulatory hormone that blocks iron export from cells to the circulation (45, 110). As a result, levels of plasma iron and transferrin saturation are high and iron progressively deposits in the liver (155, 171). *Trf*$^{hpx/hpx}$ mice have virtually no transferrin (less than 1% of normal) (172). Without transferrin, iron cannot be delivered to bone marrow. Therefore, *Trf*$^{hpx/hpx}$ mice are severely anemic, have increased iron absorption, and iron is massively loaded into tissues, including liver, heart, kidney, pancreas and adrenal gland (156). Lastly, ^{59}Fe-labeled ferric citrate, or ^{59}Fe-labeled transferrin were injected into mice through the tail vein and the uptake of hepatic ^{59}Fe was compared between *Dmt1*$^{liv/liv}$ and *Dmt1*$^{flox/flox}$ controls.

Results

Inactivation of DMT1 Specifically in the Liver

To investigate the role of DMT1 in hepatic iron uptake, mice harboring loxP recombination sites flanking exon 6 to 8 of the *Dmt1* gene (*DMT1*$^{flox/flox}$) (26) were crossed with mice carrying an Alb-cre transgene, which allows for Cre expression under the control of the liver-specific albumin promoter and inactivates DMT1 specifically in the hepatocyte (173). I confirmed the excision by PCR using F1, R1, and R2 primers, assuring the specificity of recombination in liver (Figure 3-1A,B). Quantitative RT-PCR analysis demonstrated that *Dmt1* mRNA levels were lower in the liver by > 90% in *Dmt1*$^{liv/liv}$ than in *Dmt1*$^{flox/flox}$ mice. *Dmt1* mRNA levels in heart and kidney were also

measured to ensure that expression in extrahepatic tissue was not affected (Figure 3-1C). Western blot analysis of liver lysates detected a DMT1-immunoreactive band at ~70 kDa in *Dmt1*$^{flox/flox}$, but not in *Dmt1*$^{liv/liv}$ mice, confirming DMT1 inactivation in the liver (Figure 3-1D). Iron status parameters were compared between *Dmt1*$^{flox/flox}$ and *Dmt1*$^{liv/liv}$ mice. Hemoglobin, plasma iron level, transferrin saturation and levels of hepatic total iron and nonheme iron were similar in *Dmt1*$^{flox/flox}$ and *Dmt1*$^{liv/liv}$ mice (Table 3-1). Body weight, liver weight or ratio of liver/body weight also did not differ between groups. To ensure the age groups selected in this study had efficient Cre-Lox recombination, hepatic *Dmt1* mRNA levels of *Dmt1*$^{liv/liv}$ mice were analyzed by qRT-PCR up to 16 weeks old and this confirmed a > 80% inactivation at all age groups (Figure 3-2).

Liver-specific Inactivation of *Dmt1* in *Hfe*$^{-/-}$ *or Trf*$^{hpx/hpx}$ Mice does not affect Hepatic Iron Loading or Body Iron Status

To determine if DMT1 plays a role in hepatic iron accumulation, *Dmt1*$^{liv/liv}$ mice were crossed with *Hfe*$^{-/-}$ and *Trf*$^{hpx/hpx}$ mice to generate *Hfe*$^{-/-}$*;Dmt1*$^{liv/liv}$ and *Trf*$^{hpx/hpx}$*;Dmt1*$^{liv/liv}$ mice, along with their respective controls (*Hfe*$^{-/-}$*;Dmt1*$^{flox/flox}$ and *Trf*$^{hpx/hpx}$*;Dmt1*$^{flox/flox}$) mice. Hepatic *Dmt1* mRNA levels in double-mutant *Dmt1*$^{liv/liv}$ mice were >90% lower than in the *Dmt1*$^{flox/flox}$ controls (data not shown), thus confirming inactivation of *Dmt1* in these strains.

Hfe$^{-/-}$*;Dmt1*$^{flox/flox}$ mice had increased plasma iron level, higher transferrin saturation (Figure 3-3A,B) and the hepatic nonheme iron level was 3-fold higher than that of *Dmt1*$^{flox/flox}$ mice (Figure 3-3C). Inactivation of *Dmt1* specifically in hepatocytes, however, did not affect these parameters in *Hfe*$^{-/-}$ mice. Similarly, *Trf*$^{hpx/hpx}$ mice had lower levels of hemoglobin and plasma iron (Figure 3-4A,B), and hepatic nonheme iron

level of *Trf*$^{hpx/hpx}$;*Dmt1*$^{flox/flox}$ mice was 11 times higher than that of *Dmt1*$^{flox/flox}$ mice. However, none of these parameters were different between *Trf*$^{hpx/hpx}$;*Dmt1*$^{liv/liv}$ and *Trf*$^{hpx/hpx}$;*Dmt1*$^{flox/flox}$ mice. To exclude the possibility that iron is not loaded in hepatocytes but in Kupffer cells in the liver, I performed histological analysis to stain ferric iron by using Perls' Prussian blue stain. I found that under normal conditions, hepatic iron is only detectable in Kupffer cells and that in iron overload conditions (with *Hfe* or *Trf* mutation), inactivation of DMT1 did not prevent iron loading into hepatocytes (Figure 3-3D; Figure 3-4D).

Hepatic concentrations of total iron (nonheme and heme), zinc, copper, manganese, and cobalt were also compared between *Dmt1*$^{flox/flox}$ and *Dmt1*$^{liv/liv}$ mice as single or double mutants by using ICP-MS (Table 3-2). I found only copper showed ~37% lower levels in *Hfe*$^{-/-}$;*Dmt1*$^{liv/liv}$ compared to *Hfe*$^{-/-}$;*Dmt1*$^{flox/flox}$ controls. The concentrations of other metals measured were unaffected in *Dmt1*$^{liv/liv}$ as single-mutants or as double-mutants intercrossed with *Hfe*$^{-/-}$ or *Trf*$^{hpx/hpx}$ mice, compared with their respective controls.

Effect of Liver-specific Inactivation of *Dmt1* on NTBI and TBI Uptake by the Liver

To determine if DMT1 is required for NTBI and TBI uptake by the liver, ^{59}Fe-labeled NTBI or TBI was injected into *Dmt1*$^{liv/liv}$ mice intravenously and ^{59}Fe uptake by the liver was measured. The liver took up the most NTBI among tissues measured (~60%), followed by kidney (10%), pancreas (5%) and heart (1%). There was no difference in hepatic NTBI uptake in *Dmt1*$^{liv/liv}$ mice compared with *Dmt1*$^{flox/flox}$ animals (Figure 3-5A). Similarly, when ^{59}Fe-labeled transferrin was injected into mice, the liver took up ~25% of whole-body counts, followed by ~4% kidney, < 1% in heart and pancreas. TBI uptake in *Dmt1*$^{liv/liv}$ mice was reduced by 40% in the liver (Figure 3-5B).

TfR1, TfR2 and ZIP14 (receptors or transporters that may participate in hepatic iron uptake) were analyzed by Western blotting. The levels of these proteins did not differ between *Dmt1*$^{flox/flox}$ and *Dmt1*$^{liv/liv}$ mice (Figure 3-6).

Discussion

The liver is the main organ that stores excess iron; however, the molecular mechanisms of how liver takes up iron, under physiologic or pathologic conditions, is not fully elucidated. DMT1 is the first mammalian iron transporter identified (25). The importance of DMT1 has been well-characterized in enterocytes and developing red blood cells (26, 77, 94). Studies have suggested that DMT1 may play a role in hepatic iron uptake (123, 126, 161), although it may not be the sole iron transporter/pathway by which the liver acquires iron (26, 163). I used a mouse model that had *Dmt1* inactivated specifically in hepatocytes, the major cell type in the liver, to investigate the role of DMT1 in hepatic iron uptake. My results show that total and non-heme iron levels do not differ between *Dmt1*$^{liv/liv}$ and *Dmt1*$^{flox/flox}$ controls, indicating that DMT1 is dispensable for the overall iron economy of the liver. Moreover, hepatic nonheme iron levels did not differ between *Hfe*$^{-/-}$*;Dmt1*$^{liv/liv}$ and *Hfe*$^{-/-}$*;Dmt1*$^{flox/flox}$ mice or between *Trf*$^{hpx/hpx}$*;Dmt1*$^{liv/liv}$ and *Trf*$^{hpx/hpx}$*;Dmt1*$^{flox/flox}$ mice, indicating that DMT1 is not required for hepatic iron overload characteristic of hemochromatosis or hypotransferrinemia. Plasma iron, total iron-binding capacity, transferrin saturation, and hemoglobin levels also did not differ between single- or double-mutant *Dmt1*$^{liv/liv}$ mice, suggesting that systemic iron metabolism was not affected.

Similar to *HFE*-related hemochromatosis patients, *Hfe*$^{-/-}$ mice deposit the excess iron starting with periportal hepatocytes (171) and have elevated NTBI in the plasma (126). I found a similar pattern of iron deposition in the livers of *Hfe*$^{-/-}$*;Dmt1*$^{liv/liv}$ mice,

indicating DMT1 is not required for hepatocyte iron accumulation in this animal model. Plasma NTBI is believed to be the major contributor to hepatic iron accumulation because of its elevated levels during iron overload conditions and rapid clearance by hepatocytes (126, 168). Therefore, hepatic nonheme levels did not differ between *Hfe*$^{-/-}$*;Dmt1*$^{liv/liv}$ and *Hfe*$^{-/-}$*;Dmt1*$^{flox/flox}$ mice also suggests that hepatocyte DMT1 is not required for NTBI uptake. This likelihood is strongly supported by the observation that hepatic iron deposition was not affected in *Trf*$^{hpx/hpx}$*;Dmt1*$^{liv/liv}$ mice compared to controls because *Trf*$^{hpx/hpx}$ mice have no plasma transferrin (156), therefore most iron in the plasma is NTBI.

I formally examined the role of hepatocyte DMT1 in NTBI clearance by injecting ^{59}Fe-labeled ferric citrate, the physiological form of NTBI in iron overload patients, into *Dmt1*$^{liv/liv}$ mice. I found that without hepatocyte DMT1, the liver still takes up NTBI efficiently. Similarly, previous studies of iron-loaded mice showed ~50% of NTBI uptake into the liver and ~3% to pancreas (172) and that the rank order of NTBI uptake in *Trf*$^{hpx/hpx}$ mice was liver > kidney > pancreas > heart (174). In contrast, hepatic ^{59}Fe-labeled TBI uptake was 40% lower in *Dmt1*$^{liv/liv}$ mice while other players that have been implicated in hepatic iron transport, such as TfR1, TfR2 and ZIP14 were not upregulated, indicating that DMT1 is partially required for TBI uptake.

Conversely, the fact that TBI uptake was only 40% lower in *Dmt1*$^{liv/liv}$ mice also indicated that there are other transporter(s) that can compensate for the loss of DMT1. One such possible transporter is ZIP14. A previous study showed that overexpression of ZIP14 in HEK 293T cells increased TBI uptake, whereas HepG2 cells treated with ZIP14 siRNA showed nearly a 40% decrease in TBI uptake (137). Although ZIP14

protein levels were not upregulated in *Dmt1*$^{liv/liv}$ mice, it is still a good candidate to compensate for the loss of DMT1 because its expression is 10 times higher than *Dmt1* in HepG2 cells and it mediates iron transport at pH 6.5 (137). More recently, ZIP8 was also shown to be an iron transporter that transports NTBI in HEK 293T cells and in *Xenopus* oocytes (175). Moreover, ZIP8 hypomorphic mice (which express 90% less ZIP8 than normal) had 50% lower hepatic iron levels at birth, suggesting that ZIP8 may play a role in hepatic iron transport or in maternofetal iron transfer (176).

In conclusion, these data indicate that hepatocyte DMT1 is not required for hepatic iron accumulation during normal and overload conditions or for NTBI uptake, but is partially required for efficient iron assimilation from transferrin. Further studies, including those using *Zip14* and/or *Zip8* knockout mice, are thus warranted to examine other possible pathways of hepatic iron uptake.

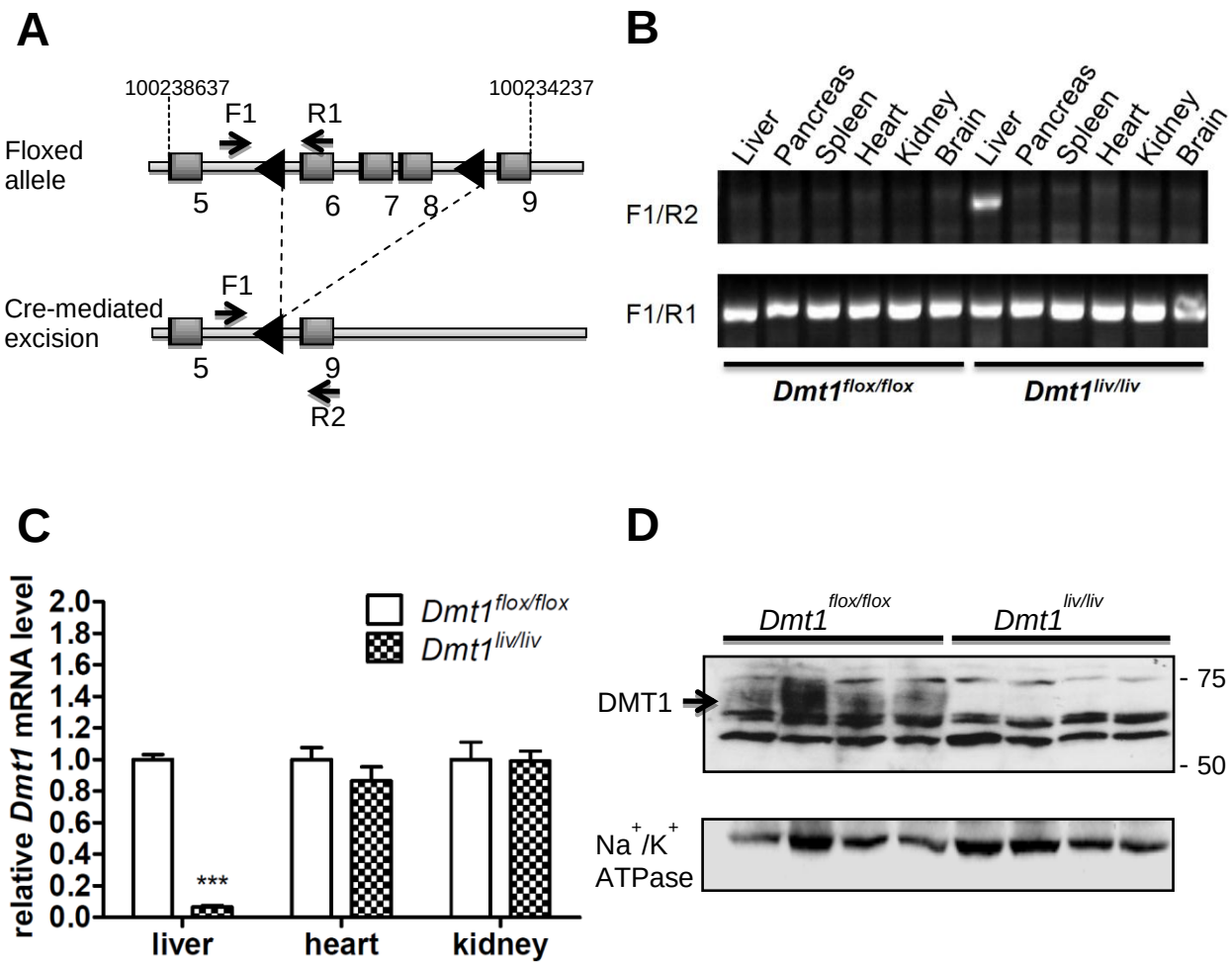

Figure 3-1. Disruption of *Dmt1* in the liver. A) Schematic depictions of the LoxP-flanked allele and conditional knockout alleles. F1, R1, and R2 indicate primers used for PCR genotyping. B) PCR analysis of genomic DNA extracted from tissues of mice at 8 weeks of age. C) Relative *Dmt1* mRNA expression in liver, heart, and kidney by using quantitative RT-PCR with *Rpl13a* as an internal control gene. Values represent mean ± SE, n=3-4, ***P<0.001. D) Western blot analysis of DMT1 in crude membrane isolated from livers of $Dmt1^{flox/flox}$ and $Dmt1^{liv/liv}$ mice. All analyses were performed on samples from 8-week-old mice.

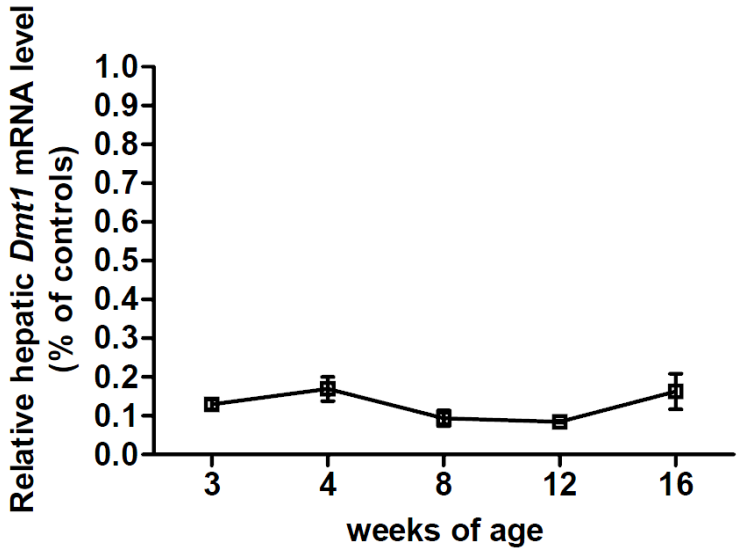

Figure 3-2. Relative *Dmt1* mRNA levels in livers of *Dmt1*$^{liv/liv}$ mice at various ages by using quantitative with *Rpl13a* as an internal control gene. Transcript levels are expressed as a percent of levels in *Dmt1*$^{flox/flox}$ control livers. Values represent mean ± SE, n=3-7.

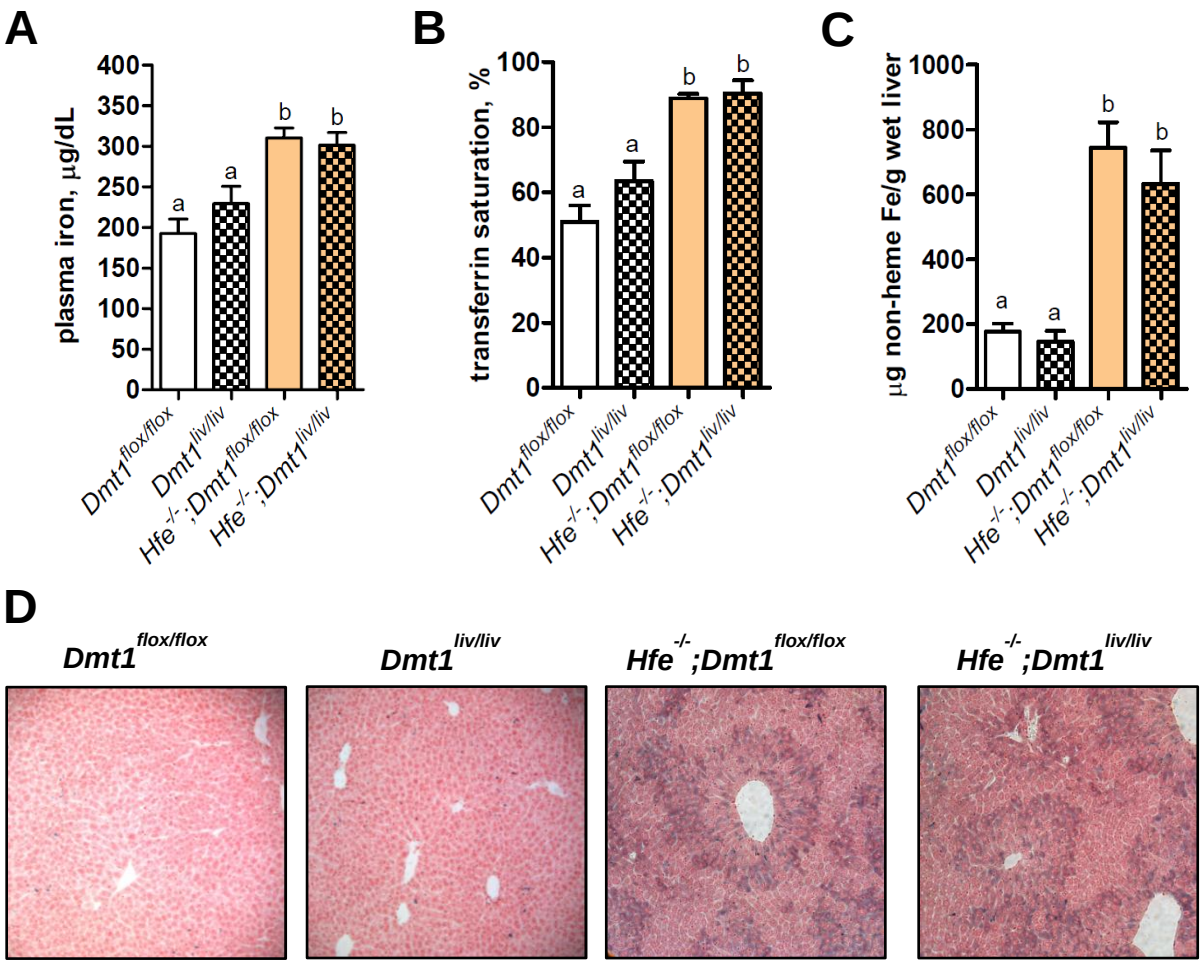

Figure 3-3. Plasma iron levels, transferrin saturation and hepatic iron accumulation are not affected by liver-specific inactivation of *Dmt1* in *Hfe*$^{-/-}$ mice. A) Plasma iron concentration and B) transferrin saturation were determined by using standard methods. C) Liver nonheme iron levels were determined colorimetrically after acid digestion of tissues. Values represent mean ± SE, n=6. Means without a common superscript differ significantly ($P < 0.05$). D) Histological examination of iron loading in the liver by using Perls' Prussian blue staining. All analyses were performed on samples from 16-week-old mice.

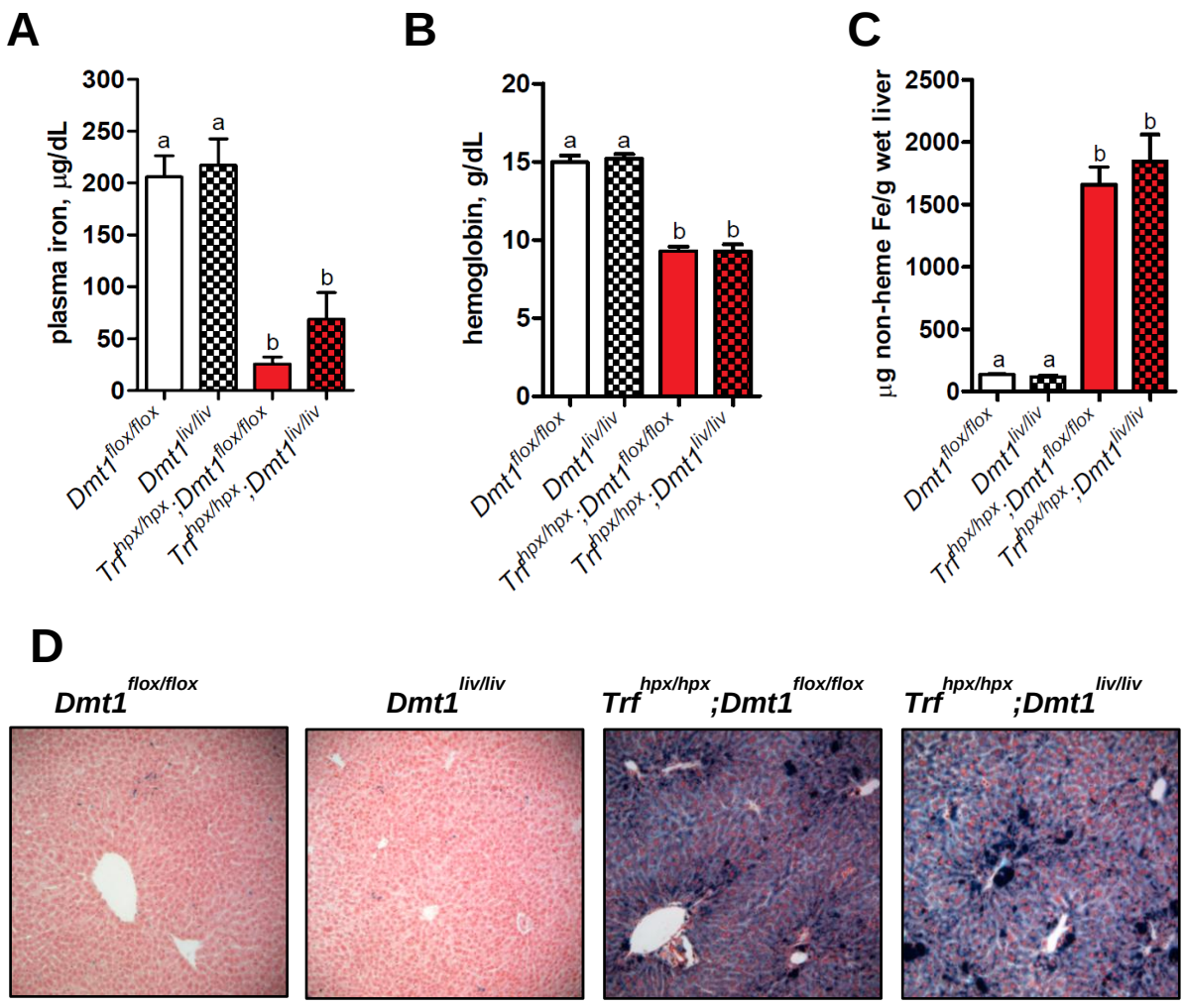

Figure 3-4. Plasma iron, hemoglobin levels and hepatic iron accumulation are not affected by liver-specific inactivation of *Dmt1* in hypotransferrinemic ($Trf^{hpx/hpx}$) mice. A) Hemoglobin and B) plasma iron concentration were determined by using standard methods. C) Hepatic nonheme iron levels were determined colorimetrically after acid digestion of tissues. Values represent mean ± SE, n=6, except for hemoglobin levels in $Trf^{hpx/hpx}$ mice (n=3-4). Means without a common superscript differ significantly ($P < 0.05$). D) Histological examination of iron loading in the liver by using Perls' Prussian blue staining. All analyses were performed on samples from 16-week-old mice.

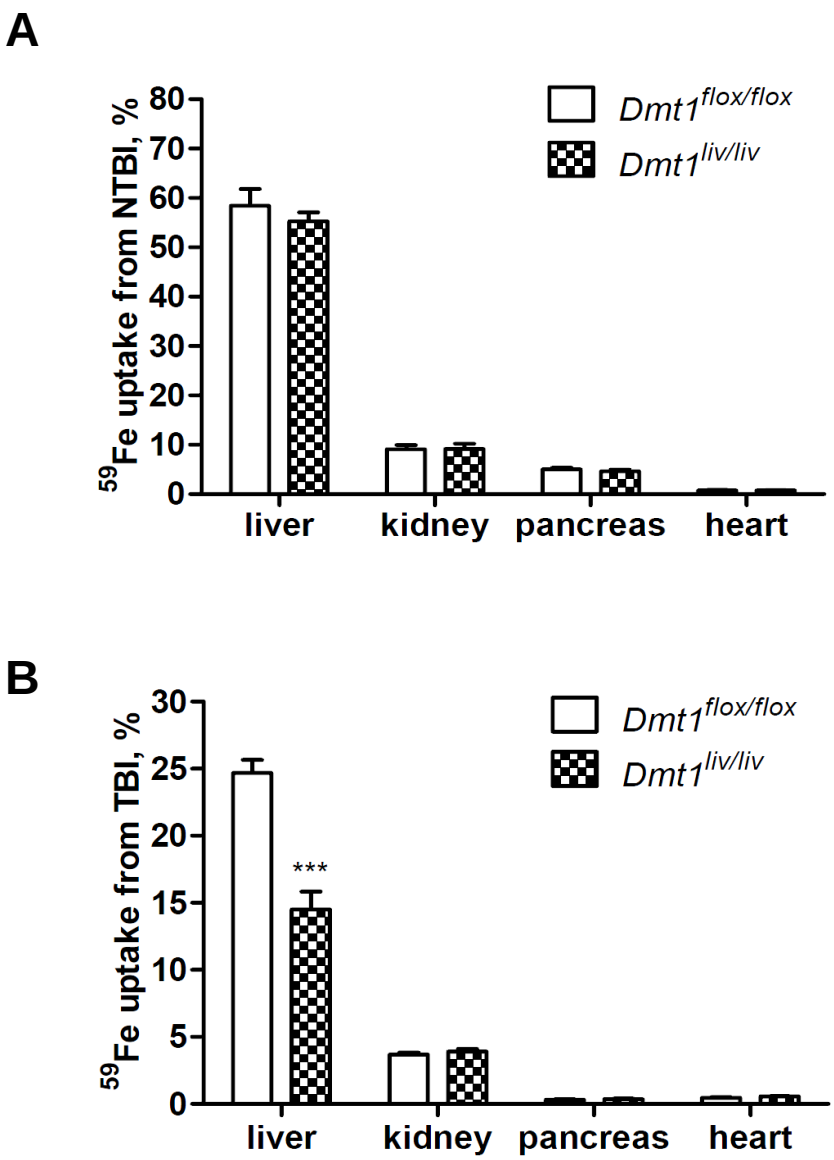

Figure 3-5. Tissue uptake of ^{59}Fe from NTBI or TBI injected into the plasma of *Dmt1*$^{flox/flox}$ and *Dmt1*$^{liv/liv}$ mice. A) NTBI uptake by the liver (n=10), kidney (n=5), pancreas (n=5) and heart (n=5). Mice were injected with ferric citrate to transiently saturate plasma transferrin and ^{59}Fe-labeled ferric citrate was injected 10 min later. After 2 h, mice were sacrificed and whole-body and tissue ^{59}Fe were determined by gamma counting. Tissue uptake of ^{59}Fe from NTBI was calculated as a percentage of whole-body cpm. B) TBI uptake by the liver (n=14), kidney (n=6), pancreas (n=6) and heart (n=6). Mice were injected with ^{59}Fe-transferrin and sacrificed after 2 h. Whole-body and tissue ^{59}Fe were determined by gamma counting. Tissue uptake of ^{59}Fe from TBI was calculated as a percentage of whole-body cpm. Values represent mean ± SE. All measurements were performed on mice at 8-week-old.

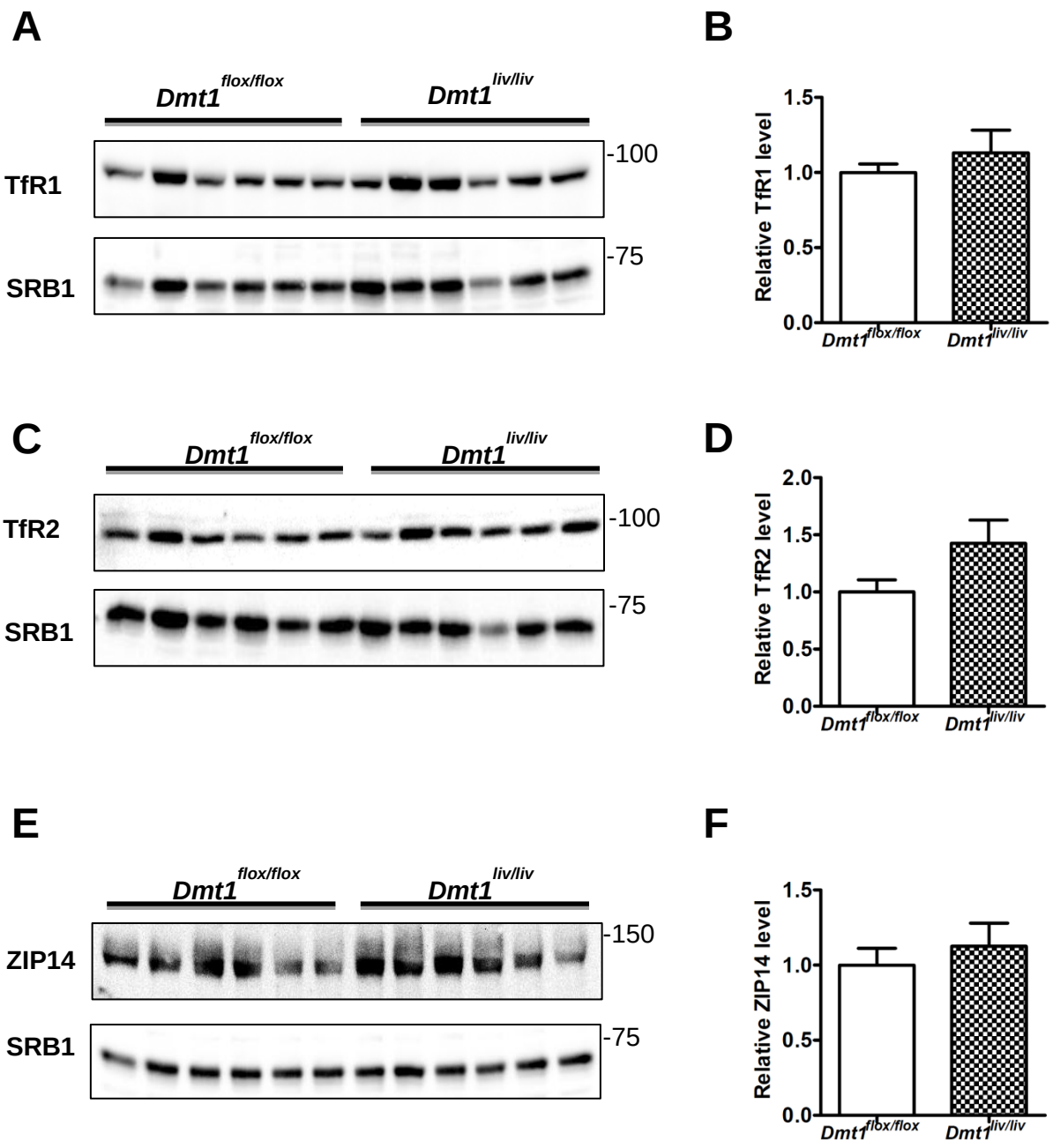

Figure 3-6. Effect of liver-specific inactivation of *Dmt1* on hepatic levels of TfR1, TfR2, and ZIP14. A) Western blot analysis of TfR1 and B) the quantification by densitometry in livers of $Dmt1^{flox/flox}$ and $Dmt1^{liv/liv}$ mice. C) Western blot analysis of TfR2 and D) the quantification by densitometry. E) Western blot analysis of ZIP14 and F) the quantification by densitometry. Blots were stripped and reprobed for SR-B1. Values represent mean ± SE, n=6. All analyses were performed on samples from 8-week-old mice.

Table 3-1. Iron status parameters of *Dmt1*$^{flox/flox}$ and *Dmt1*$^{liv/liv}$ mice

Parameter	Units	*Dmt1*$^{flox/flox}$	*Dmt1*$^{liv/liv}$	*n*	*P*
Body weight	g	19.98 ± 0.56	19.55 ± 0.47	6	0.565
Liver weight	g	0.83 ± 0.07	0.81 ± 0.04	6	0.873
Hemoglobin	g/dL	15.30 ± 0.33	15.18 ± 0.47	6	0.843
Plasma iron level	µg/dL	270.32 ± 17.72	283.56 ± 14.44	6	0.575
TIBC	µg/dL	372.63 ± 15.01	375.00 ± 27.72	4-5	0.938
Transferrin saturation	%	72.36 ± 4.25	73.88 ± 3.69	4-5	0.802
Hepatic total iron	µg Fe/g	796.70 ± 65.08	885.00 ± 12.66	3	0.254
Hepatic nonheme iron	µg Fe/g	132.12 ± 22.24	125.92 ± 26.24	6	0.861

TIBC, total iron-binding capacity. Hepatic iron (heme and nonheme) levels were determined by ICP-MS, and are reported as µg Fe/g of tissue dry weight. Hepatic nonheme iron levels were measured colorimetrically and are reported as µg Fe/g of tissue wet weight. Values are means ± SE. Measurements were at 8 weeks of age. *P* values were obtained by using Student's *t* test.

Table 3-2. Liver mineral concentrations in *Dmt1*$^{liv/liv}$, *Hfe*$^{-/-}$;*Dmt1*$^{liv/liv}$, and *Trf*$^{hpx/hpx}$;*Dmt1*$^{liv/liv}$ mice and their respective *Dmt1*$^{flox/flox}$ controls

	WT		*Hfe*$^{-/-}$		*Trf*$^{hpx/hpx}$	
	Dmt1$^{flox/flox}$	*Dmt1*$^{liv/liv}$	*Dmt1*$^{flox/flox}$	*Dmt1*$^{liv/liv}$	*Dmt1*$^{flox/flox}$	*Dmt1*$^{liv/liv}$
Fe	507.8 ± 82.7	468.8 ± 100.6	1911 ± 175.6	2503 ± 540.4	4656 ± 690.1	4369 ± 549.0
Zn	94.17 ± 5.43	105.0 ± 2.79	102.3 ± 2.50	122.0 ± 12.54	109.7 ± 4.57	96.60 ± 8.18
Cu	29.50 ± 6.23	41.17 ± 5.49	40.50 ± 5.01	25.50 ± 1.86*	20.17 ± 1.35	18.20 ± 0.73
Mn	3.87 ± 0.41	3.93 ± 0.25	3.90 ± 0.07	3.25 ± 0.29	4.25 ± 0.31	3.22 ± 0.53
Co	0.16 ± 0.01	0.19 ± 0.01	0.16 ± 0.01	0.18 ± 0.02	0.17 ± 0.01	0.14 ± 0.01

Liver mineral concentrations (ppm) were determined by ICP-MS. Values are means ± SE of 5-6 mice per group. Comparisons between *Dmt1*$^{flox/flox}$ and *Dmt1*$^{liv/liv}$ mice as single or double mutants, were performed by using Student's *t* test, **P* < 0.05. Measurements were at 16 weeks of age.

CHAPTER 4
CHARACTERIZATION OF ZIP8 AS A NOVEL IRON TRANSPORTER

Introduction

Iron is an essential metal to life yet too much is toxic. Iron homeostasis needs to be tightly regulated; however, the molecular detail of how iron gets into mammalian tissues is not fully understood except for two cell types: enterocytes and developing erythroid cells. It is well established that DMT1 is required in both cell types. In enterocytes, iron is reduced to the ferrous form before it can be taken up by DMT1 at the brush-border membrane (25, 26). In developing erythroid cells, DMT1 is essential for releasing iron from endosomes to cytoplasm (77, 79). Studies of *Dmt1*$^{-/-}$ mice revealed that iron accumulated in the liver, suggesting DMT1 is not required in materno-fetal transfer and that there is at least one DMT1-independent iron transport pathway in the liver (26). One such pathway may involve ZIP14, which has been shown to mediate the uptake of NTBI and to localize to the plasma membrane of hepatocytes (135). ZIP14 belongs to the ZIP superfamily of transmembrane proteins that are responsible for zinc transport into cells. Functional studies using the *Xenopus laevis* oocyte heterologous expression system showed that ZIP14-mediated iron uptake was optimal at pH 7.5 (136), consistent with the implication that ZIP14 may play a role in NTBI uptake in the liver and in contrast to DMT1, which mediates iron uptake optimally at pH 5.5 (25). In the ZIP superfamily, ZIP8 shares high homology with ZIP14 (~50% amino acid identical). ZIP8 has been shown to transport zinc, cadmium and manganese (138, 140),

---

Reprinted with permission from 177. Wang CY, Jenkitkasemwong S, Duarte S, Sparkman B, Shawki A, Mackenzie B, Knutson MD. ZIP8 Is an Iron and Zinc Transporter Whose Cell-surface Expression Is Upregulated by Cellular Iron Loading. J Biol Chem 2012.

but the capability of ZIP8 to transport iron has not been reported. Given that ZIP8 shares high homology with ZIP14, I investigated the possibility that ZIP8 functions as an iron transporter.

Results

Overexpression of ZIP8 Increases Cellular Uptake of Zinc and Iron

To determine if ZIP8 transports iron in addition to zinc, I transiently overexpressed rZIP8 in HEK293T cells and measured the uptake of ^{59}Fe-ferric citrate in the presence of 1 mM ascorbate. Overexpression of ZIP8 was confirmed by Western blotting (Figure 4-1A). The data showed a two-fold increase in iron uptake and a 45% increase in zinc uptake in cells overexpressing ZIP8 (Figure 4-1B). When 10-fold molar excess of unlabeled zinc was added to the medium, >90% of iron uptake activity was inhibited. Likewise, 10-fold molar excess iron inhibited zinc uptake (Figure 4-1C).

ZIP8-mediated Iron Transport Activity is pH-Dependent

To determine the pH dependence of ZIP8-mediated iron transport, iron uptake was measured in medium at pH 7.5, 6.5, or 5.5 in HEK293T cells overexpressing mZIP8. ZIP8-mediated iron transport occurs at both pH 7.5 and 6.5, but not at pH 5.5 in HEK293T transfected cells (Figure 4-2).

ZIP8 is Glycosylated and Detectable at the Cell Surface in H4IIE Cells

The observation that ZIP8-mediated iron transport activity at pH 7.5 and 6.5 led me to characterize ZIP8 in H4IIE rat hepatoma cells because hepatocytes take up NTBI (126) and TBI (178), at pH 7.5 and 6.5, respectively. By immunoprecipitation, the major ZIP8-immunoreactive band in H4IIE cells is at approximately 140 kDa (Figure 4-3A), which is greater than the predicted molecular mass of 50 kDa. To determine if endogenous ZIP8 is glycosylated, I blocked endogenous glycosylation by treating H4IIE

cells with tunicamycin and further removed existing *N*-linked glycans by treating lysates with PGNase F. ZIP8 shifted down to 100 kDa when treated cells with tunicamycin and to 75 kDa when PNGase F was added into lysates (Figure 4-3B). To determine if ZIP8 is detectable at the cell surface, I isolated the biotinylated fraction of H4IIE cells followed by Western blotting. The data suggested that the 140 kDa form of ZIP8 is the predominant, glycosylated form present at the cell surface (Figure 4-3C).

ZIP8 Protein Expression is Induced upon Iron Treatment in H4IIE Cells

To determine if ZIP8 is regulated by iron, H4IIE cells were treated with 100 or 250 μM Fe-NTA for 72 h and protein expression was examined by Western blotting. Iron treatment increased ZIP8 levels in both total cell lysates and cell-surface fractions (Figure 4-4A). It is well established that TfR1 expression decreases during iron-loaded conditions (179), and thus it was used as an iron loading indicator. SR-BI was probed to demonstrate the enrichment of the cell surface biotinylated fraction and the equivalent lane loading. CCS is a cytosolic protein, thus indicating that the isolated cell-surface biotinylated fraction was not contaminated with cytosolic proteins and that total cell lysates were equally loaded (Figure 4-4A). I next examined whether ZIP8 expression is also regulated by zinc by treating H4IIE cells with 40 μM zinc chloride ($ZnCl_2$) for 3 h or 48 h. ZIP8 protein expression was induced by 3 h $ZnCl_2$ treatment but not 48 h (Figure 4-4B).

Tissue Expression of ZIP8, ZIP14 and DMT1

To compare tissue expression of ZIP8 with other known mammalian iron transporters — ZIP14 and DMT1—I determined the copy number for each gene from pooled human total RNA. Among 20 different tissues examined, ZIP8 is most abundant in lung, placenta, salivary gland, and thymus and lowest in skeletal muscle, fetal brain,

and testis. ZIP14 is most abundant in liver, heart, thyroid gland, and small intestine, whereas DMT1 is most abundant in cerebellum, thymus, prostate and kidney (Figure 4-5).

Suppression of ZIP8 Expression in BeWo Cells

To assess iron transport capability of endogenous ZIP8, I suppressed ZIP8 expression by using siRNA targeting *ZIP8* mRNA and measured iron transport activity in BeWo cells, a placental cell line derived human choriocarcinoma. In BeWo cells treated with ZIP8 siRNA, ZIP8 protein expression was suppressed by 90% and iron transport activity was decreased by 37%, compared to control cells treated with negative control siRNA (Figure 4-6).

Discussion

In this chapter, I have demonstrated that ZIP8 can mediate cellular iron transport, making it the third mammalian iron import protein to be identified. ZIP8 was first cloned from monocytes that were induced during innate immune activation stimulated by *Mycobacterium bovis* BCG cell wall and the induction increased intracellular zinc concentrations (138). It was later found to be responsible for cadmium toxicity in testis and kidney (139, 146). Here, I showed that ZIP8 can mediate cellular iron transport, in addition to zinc, and the presence of excessive unlabeled zinc or iron showed mutual inhibition of the uptake activity, suggesting that the transport pathway mediated by ZIP8 is shared by zinc and iron. Treatment of H4IIE cells with iron increased ZIP8 expression at the cell surface, suggesting ZIP8 is regulated by iron. Treatment of H4IIE cells with zinc also increased ZIP8 expression; however, the effect was transient. The fact that ZIP8 expression is upregulated at the cell surface by iron loading and that ZIP8 is an

iron/zinc transporter may explain hepatic zinc accumulation during iron overload conditions (141, 180, 181).

DMT1 is the best characterized mammalian iron transporter thus far, and it is widely cited to be responsible for NTBI uptake in the liver (163, 165, 168, 182). However, my studies indicate that hepatocyte DMT1 is dispensable for hepatic NTBI uptake. It is established that ZIP14 can mediate NTBI uptake by overexpressing mZIP14 in HEK 293H and Sf9 insect cells (135). Considering that DMT1-mediated iron uptake was optimal at pH 5.5, but poor at pH 7.5 (25), and that ZIP14-mediated iron uptake is optimal at pH 7.5 (136), makes ZIP14 a promising candidate for hepatic NTBI uptake. Similar to ZIP14, ZIP8-mediated iron uptake occurs at pH 7.5 and 6.5, but not at 5.5, indicating that ZIP8 may facilitate NTBI clearance from blood into tissues and/or playing a role in iron assimilation from TBI, but unlikely to mobilize iron from lysosomes, where it has been detected previously (138, 145).

Although ZIP8 mediates iron uptake at pH 7.5 and is detectable at the surface of H4IIE cells, according to its expression profile, it is not abundant in the liver or heart, the iron-susceptible organs in iron overload, but in lung and placenta. Others reported its expression is high in pancreas (138), which was not included in the human total RNA master panel I used. Nonetheless, a microarray study using hearts from beta-thalassemic mice showed a 1.8-fold increase in ZIP8 expression and in contrast, DMT1 showed a 1.7 fold decrease (183), suggesting ZIP8 may be playing a role in NTBI uptake in beta-thalassemic hearts. According to the tissue expression profile, ZIP8 is abundant in placenta and iron uptake activity was decreased by 37% in BeWo cells treated with ZIP8 siRNA, raising the possibility that ZIP8 plays a role in maternofetal

iron transfer *in vivo*. This seems even more plausible considering that the other two known iron-import proteins, DMT1 and ZIP14, are dispensable for iron transfer across the placenta (26, 184). Studies of ZIP8 hypomorph mice revealed that homozygotes died between gestational day 18.5 and postnatal 48 h (176). Moreover, hemoglobin, hematocrit and RBC levels were significantly decreased at gestational day 16.5 and hepatic iron and zinc levels were decreased at postnatal day 1 (176), indicating ZIP8 may play an important role in placental iron transfer and possibly hepatic iron uptake.

In conclusion, ZIP8 is the third mammalian iron importer to be identified. Whether it plays an important role in placental iron transfer under physiologic conditions and/or NTBI uptake during iron overload in iron susceptible organs such us liver, heart, and pancreas, needs to be further investigated by using tissue-specific knockout mouse models.

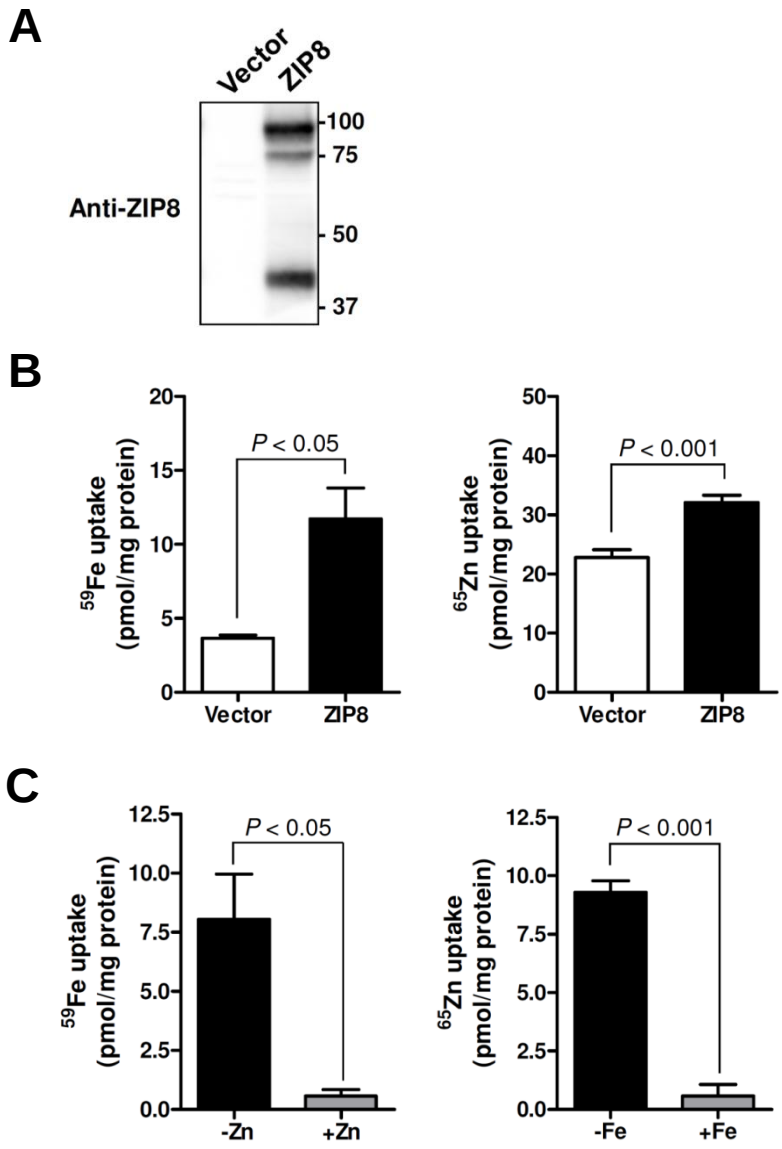

Figure 4-1. Overexpression of ZIP8 increases the cellular uptake of iron and zinc. A) Western blot analysis of ZIP8 in total cell lysates of HEK 293T cells transiently transfected with empty pExpress vector or pExpress-rat ZIP8. B) Cellular uptake of iron and zinc in HEK 293T cells overexpressing ZIP8. Forty-eight hours after transfection, cells were incubated for 1 h in uptake medium containing 2 µM ^{59}Fe-ferric-citrate or ^{65}Zn-$ZnCl_2$, and cellular uptake of ^{59}Fe (left) or ^{65}Zn (right) was measured by gamma counting. C) Mutual inhibition of iron and zinc uptake in cells overexpressing ZIP8. ^{59}Fe and ^{65}Zn uptake were measured in the presence of a 10-fold molar excess of unlabeled zinc (left) or iron (right). The amount of ^{59}Fe or ^{65}Zn taken up by cells is expressed as pmol/mg protein. Data represent the mean ± S.E. of three independent experiments. Treatment group means were compared by unpaired Student's *t* test.

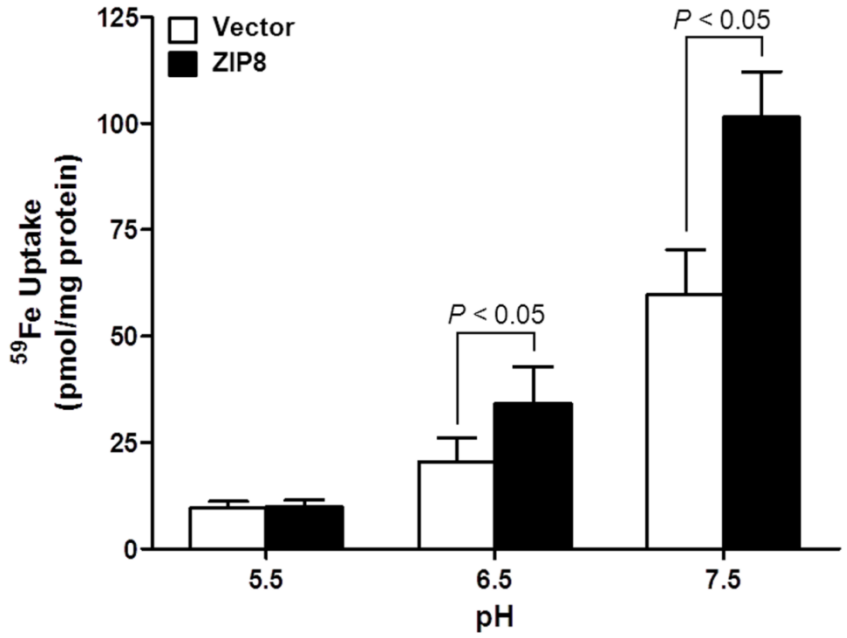

Figure 4-2. pH dependence of ZIP8-mediated iron transport. HEK 293T cells were transfected with empty pCMV-Sport6 vector or pCMV-Sport6-mouse ZIP8. Forty-eight h after transfection, cells were incubated with 2 µM ^{59}Fe-ferric citrate for 1 h in uptake buffer at pH 5.5, 6.5 and 7.5. The amount of ^{59}Fe taken up by cells is expressed as pmol/mg of protein. Data represent the mean ± S.E. of three independent experiments.

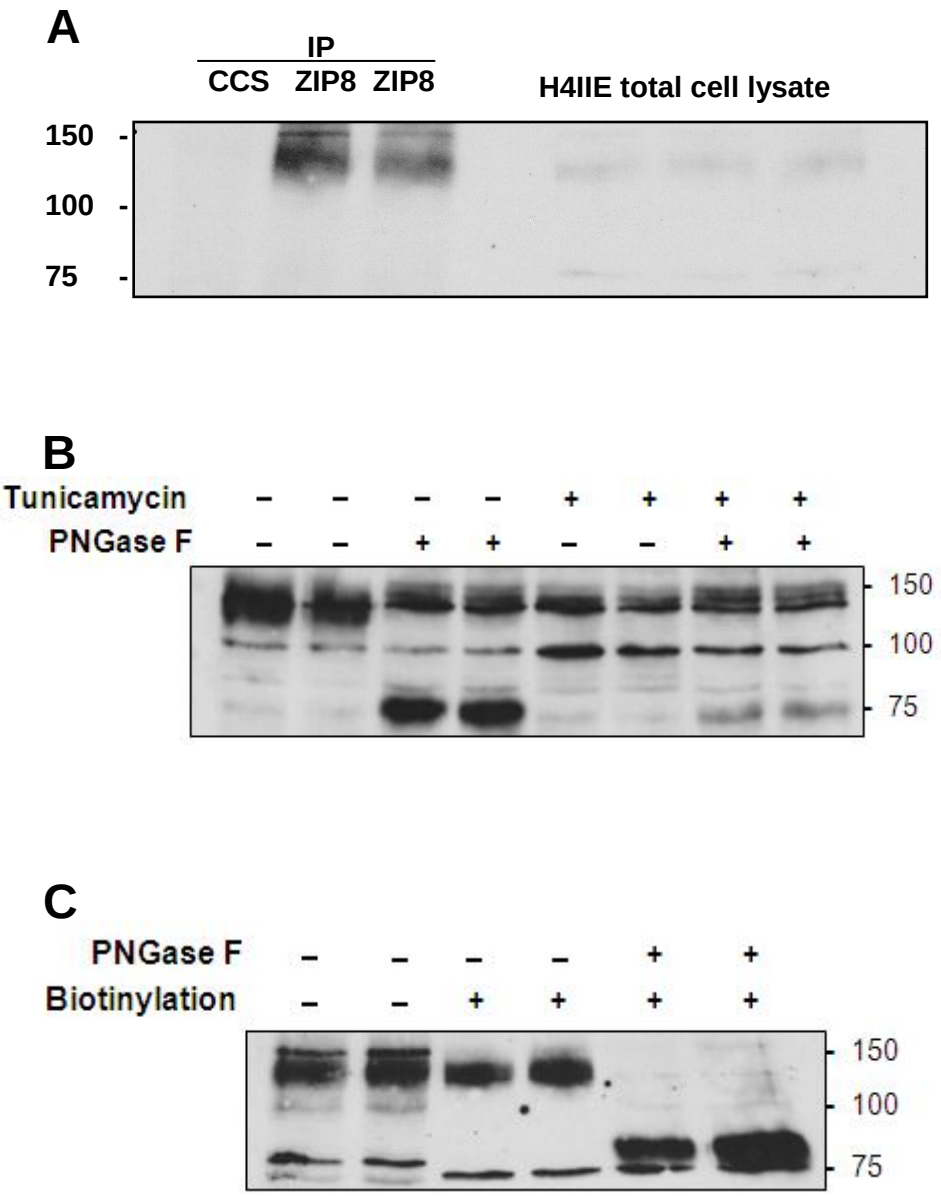

Figure 4-3. Immunoprecipitation and glycosylation analysis of endogenous ZIP8 in H4IIE rat hepatoma cells. A) Immunoprecipitation of ZIP8 followed by SDS-PAGE and immunoblotting in H4IIE total cell lysates. B) Western blot analysis of endogenous ZIP8 in H4IIE cells/cell lysates treated without (-) or with (+) tunicamycin or PNGase F. C) Western blot analysis of cell-surface ZIP8 in H4IIE cell lysates treated without (-) or with (+) PNGase F. Cell-surface proteins were labeled with Sulfo-NHS-SS-Biotin and affinity purified by using streptavidin agarose prior to Western analysis.

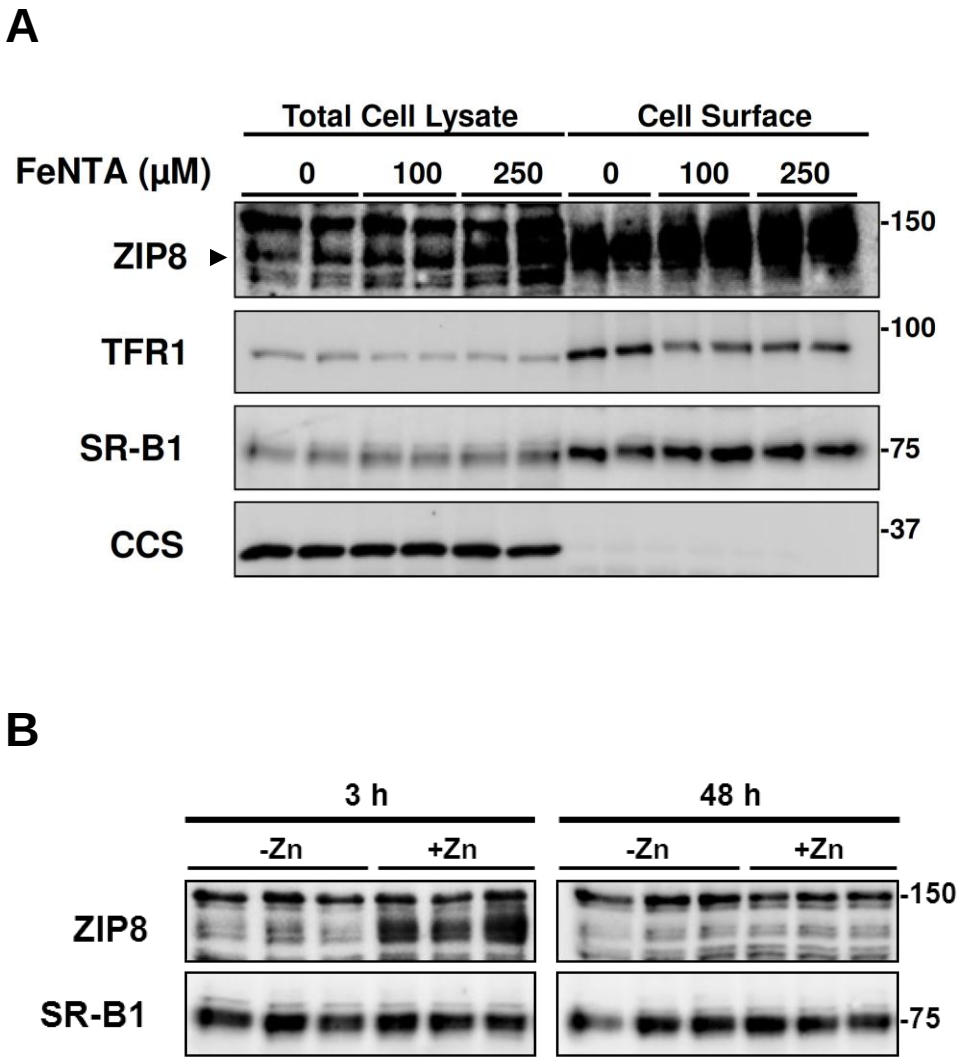

Figure 4-4. Iron and zinc loading increases ZIP8 levels in H4IIE rat hepatoma cells. A) Western blot analysis of ZIP8, TfR1, SR-B1, and CCS in total cell lysate and cell-surface proteins isolated from cells treated for 72 h with 0, 100, or 250 μM FeNTA. Cell-surface proteins were labeled with Sulfo-NHS-SS-Biotin and affinity purified by using streptavidin agarose prior to Western analysis. B) Western blot analysis of ZIP8 and SR-B1 in total cell lysates from H4IIE cells treated for 3 h and 48 h with 40 μM $ZnCl_2$.

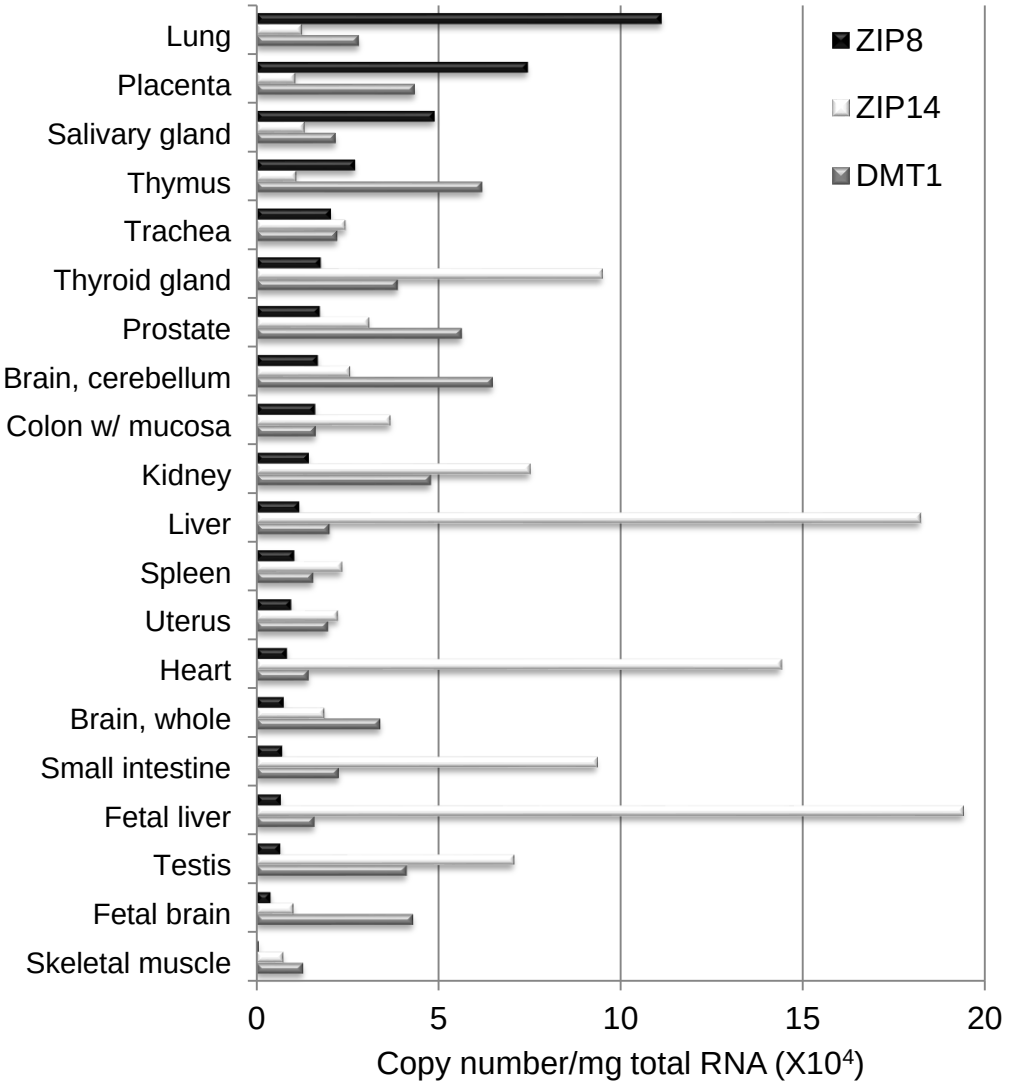

Figure 4-5. Tissue expression of *ZIP8*, *ZIP14*, and *DMT1*. Tissue expression profiles were determined by using the Human Total RNA Master Panel II derived from 20 different tissues (Clontech). Transcript copy numbers were determined by using quantitative RT-PCR.

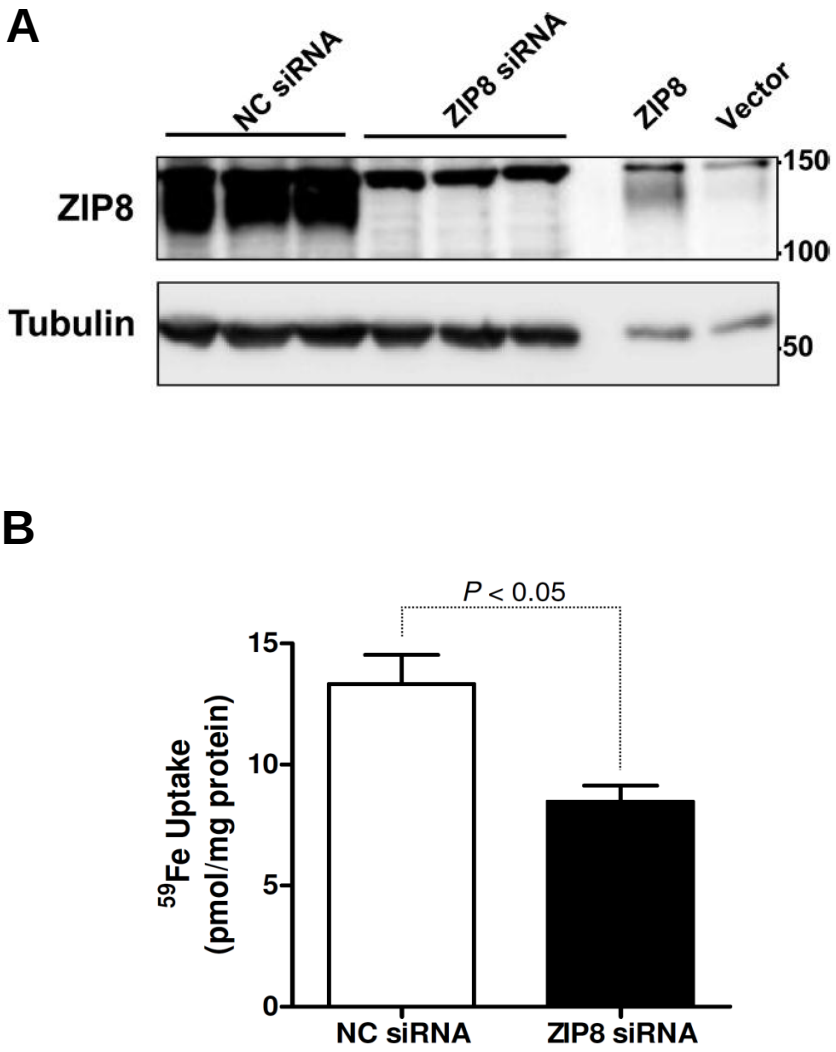

Figure 4-6. Suppression of ZIP8 expression decreases iron uptake in BeWo cells. A) Western blot analysis of lysates from BeWo cells treated with negative control (NC) siRNA or siRNA targeting *ZIP8* mRNA. As a positive control for ZIP8, BeWo cells were transfected with pCMV-Sport6 human ZIP8 cDNA (ZIP8) or empty pCMVSport6 vector (Vector). B) Cellular ^{59}Fe uptake in BeWo cells transfected with negative control (NC) siRNA or siRNA targeting *ZIP8* mRNA. Data represent the mean ± S.E. of three independent experiments.

CHAPTER 5
CONCLUSIONS, LIMITATIONS, AND FUTURE DIRECTIONS

Conclusions

The first part of my dissertation was to test the hypothesis that DMT1 plays a role in hepatic iron uptake and accumulation. I tested this hypothesis by using DMT1 hepatocyte-specific knockout mice and by crossing them with two mouse models of genetic iron overload. I found that hepatic total iron, nonheme iron concentrations, and other iron status parameters including hemoglobin, plasma iron, and TIBC were not affected by the inactivation of DMT1 specifically in hepatocytes, indicating that DMT1 is not required for hepatic iron accumulation under normal or iron overload conditions. I also injected ^{59}Fe-labeled NTBI and ^{59}Fe-labeled TBI into mice intravenously to evaluate iron uptake activities by the liver through these two pathways. Consistent with DMT1 not being required for hepatic iron accumulation, NTBI clearance by the liver was not affected in *Dmt1*$^{liv/liv}$ mice. Although I did find that DMT1 was partially required for hepatic iron uptake from transferrin (i.e. 40% lower in livers of *Dmt1*$^{liv/liv}$ mice), the contribution of this pathway to the overall iron economy of the liver is minor as hepatic iron concentration was unaffected in the knockout animals.

The second part of my dissertation tested the hypothesis that ZIP8 transports iron and investigated its regulation by iron and zinc as well as the tissue distribution. I found that overexpression of ZIP8 in HEK293T cells increased both zinc and NTBI uptake and that a 10-fold molar excess zinc inhibited iron uptake by 90%. Zinc uptake was likewise inhibited by iron, suggesting iron and zinc share a single common pathway. Cell-surface ZIP8 is upregulated by iron loading in H4IIE cells and ZIP8 mediates NTBI uptake at pH 7.5 and pH 6.5, suggesting that ZIP8 may contribute to NTBI clearance from plasma

into tissues and/or participate in iron assimilation from transferrin. By screening ZIP8 mRNA levels from 20 different tissues, I found that ZIP8 was most abundantly expressed in the lung and placenta. Moreover, siRNA-mediated suppression of ZIP8 expression in BeWo cells decreased NTBI uptake by 37%. These data reveal ZIP8 as a novel iron transporter that may play a role in iron metabolism, possibly in hepatic iron accumulation and/or in placental iron transport.

Apparent Discrepancies with the Literature

My finding that DMT1 is dispensable for NTBI uptake directly challenges the commonly held assumption that DMT1 plays a role in hepatic iron accumulation. The most cited evidence that DMT1 plays a role in hepatic iron accumulation was that DMT1 staining in rat liver was stronger in iron-loaded animals and diminished in an iron-deficient group (123) and that NTBI uptake, along with DMT1 protein expression, was increased in primary hepatocytes from *Hfe*$^{-/-}$ mice (126). However, the validation of the anti-DMT1 antibody used in these two studies was not shown, raising the question of specificity of the antibody. Moreover, in the studies of *Hfe*$^{-/-}$ mice, the authors concluded that DMT1 protein levels in isolated hepatocytes of *Hfe*$^{-/-}$ mice were two-fold higher than that of control animals, but the immunoblots were shown without proper lane loading controls and the conclusion was made by normalizing the hepatocyte expression of DMT1 from *Hfe*$^{-/-}$ mice to the levels from control mice. Another often-cited study that supports a role for DMT1 in NTBI uptake was in HLF cells, which showed that DMT1 overexpression led to an increase in ferrous iron uptake (161). However, it was also shown that in HLF cells loaded with ferric ammonium citrate, DMT1 localized mainly in the cytoplasm but not plasma membrane (161), where it would need to be to function in NTBI uptake during iron overload. Moreover, it is uncertain how relevant

overexpression systems are to normal physiology, especially since DMT1 levels in liver are usually very low (25, 75).

Limitations

There are some limitations in my studies. First, I assessed the role of DMT1 in NTBI uptake by using normal mice, which have very little, if any, NTBI. Perhaps it would have been better to assess hepatic NTBI uptake in *Hfe*$^{-/-}$ mice, for they have been reported to have elevated DMT1 levels in hepatocytes (although I have not been able to verify this using whole liver). So, if I compare NTBI clearance in these iron-loaded animals (*Hfe*$^{-/-}$*;Dmt1*$^{flox/flox}$ and *Hfe*$^{-/-}$*;Dmt1*$^{liv/liv}$), I might see a difference. Second, I only evaluated iron concentrations at two time points – 8 weeks and 16 weeks. It is known that iron status varies with age (185), and I did find a 100% increase in hepatic TfR1 levels in *Dmt1*$^{liv/liv}$ mice at age of 16 weeks, but not 8 weeks (data not shown). Lastly, I used both male and female mice for all analysis. Compared to male mice, females tend to have higher hepatic iron stores that contributed to higher variation in this study and thus would be more difficult to see difference with n=6. The major limitation of the ZIP8 project was that the study was performed exclusively in cell culture models. Future studies using whole animals will be required to define the *in vivo* role of ZIP8 in iron metabolism, especially in the liver and placenta.

Future Directions

The conclusion from DMT1 project suggested two directions. First, as DMT1 is dispensable for hepatic iron uptake and accumulation, studies using *Zip14* and/or *Zip8* knockout mice are thus warranted to examine other possible pathways of hepatic iron accumulation. Second, the fact of DMT1 is partially required for TBI uptake but hepatic iron levels did not differ suggested that under normal conditions, the major contributor of

hepatic iron source is not from TBI. As liver can also acquire iron from other pathways, such as heme-hemopexin, hemoglobin-haptoglobin, ferritin, and lactoferrin (163), future experiments will be needed to take these pathways into consideration to elucidate hepatic iron metabolism.

With respect to the ZIP8 project, studies using *Zip8*$^{-/-}$ and *Zip8*$^{flox/flox}$*;Meox2 Cre*, which will inactivate ZIP8 in all tissues except extramebryonic visceral endoderm and placenta, are needed to examine the role of ZIP8 in placental iron transfer. Whether ZIP8 plays an important role during iron overload in iron susceptible organs such us liver, heart, and pancreas, also needs to be further investigated by using tissue-specific knockout mouse models.

APPENDIX A
REGULATION OF ZIP14 BY IRON OVERLOAD

ZIP14 has been implicated in NTBI uptake. I measured ZIP14 expression in iron susceptible organs, namely liver, pancreas and heart of rats fed with iron deficient (10 ppm), adequate (50 ppm) and overload (18916 ppm) as well as in liver and pancreas of Hpx mice, a genetic mouse model of iron overload. Levels of nonheme iron in rat tissues were confirmed elsewhere. Briefly, hepatic nonheme iron levels of iron-loaded rat were 60-fold higher than that of adequate group, whereas iron-deficient rats had 60% lower hepatic nonheme iron concentrations than iron-adequate animals. In iron-loaded rats, nonheme iron levels in pancreas and heart were 300% and 50% higher, respectively, than those in iron-adequate controls. In pancreas or heart, nonheme iron concentrations did not differ between iron-deficient and iron-adequate animals. Hepatic nonheme concentration of Hpx mice were 11-fold higher than that of WT mice (1658 ±142 μg/g v.s.135 ± 3.0 μg/g) whereas pancreatic nonheme levels of Hpx mice were 5-fold higher than that of WT mice (191 ± 21 μg/g v.s. 29.4 ± 3.0 μg/g).

To validate the anti-ZIP14 antibody, I used tissues from WT, *Zip14*$^{-/-}$ mice, and rats. The major ZIP14-immunoreactive band in livers from WT mice and rat was detected at approximately 130 kDa along with a smear of high-molecular-mass bands likely representing glycosylated oligomers, consistent with previous findings (184). The band at 130 kDa is not detected in livers from *Zip14*$^{-/-}$ mice thus confirming that this band is ZIP14. ZIP14 in pancreas and heart was also detected at 130 kDa (Figure A-1).

Reprinted with permission from Nam H, Wang CY, Zhang W, Hojyo S, Fukada T, Knutson MD. ZIP14 and DMT1 in the liver, pancreas, and heart are differentially regulated by iron deficiency and overload: implications for tissue iron uptake in iron-related disorders. Haematologica. Under review.

By immunoblotting, I demonstrated that ZIP14 in liver and pancreas of iron overload rat were 100% and 70% higher than that of adequate controls (Figure A-2) and that in Hpx liver, levels of ZIP14 were 50% higher than that of WT livers (Figure A-3). The up-regulation of ZIP14 by iron loading in iron-loaded rat liver and pancreas and in the livers of Hpx mice suggests it may contribute to NTBI uptake in iron overload disorders.

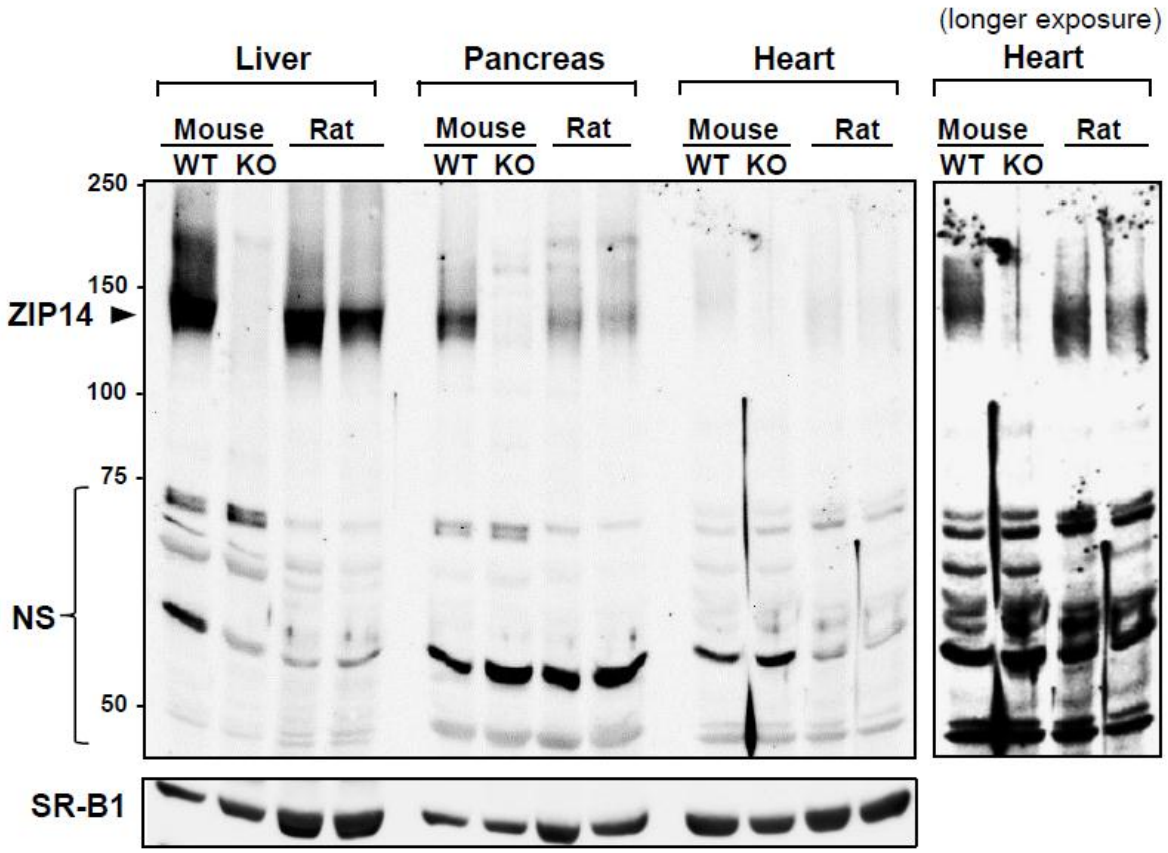

Figure A-1. Validation of the immunoreactivity of anti-ZIP14 antibody. Lysates of liver, pancreas and heart from wildtype (WT) and ZIP14 knockout (KO) mice and rat fed with iron-adequate diet were analyzed by Western blotting. The ZIP14-specific (arrowhead) and non-specific (NS) immunoreactive bands are indicated. To indicate lane loading, the blot was stripped and reprobed with the integral membrane protein SR-B1.

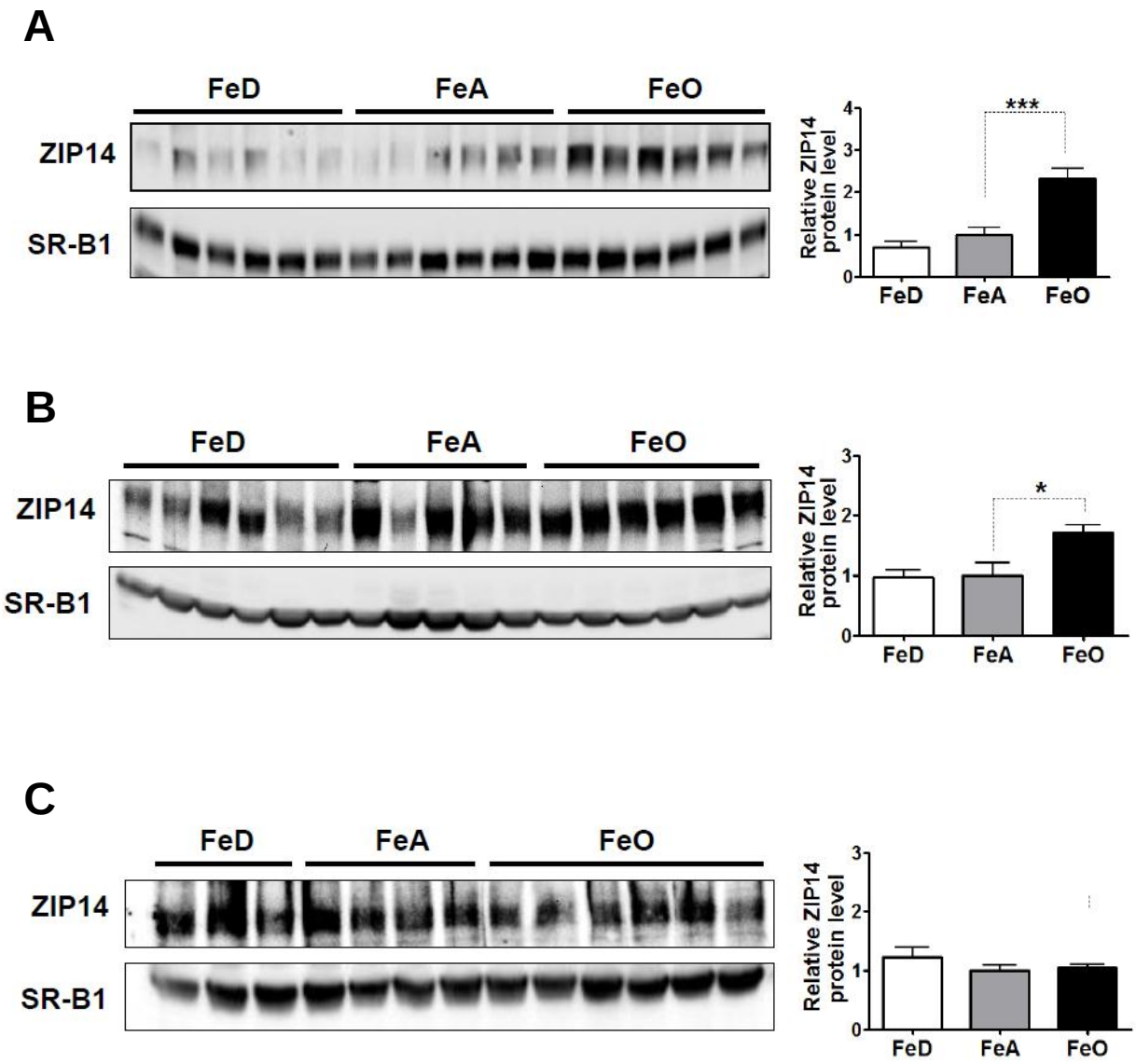

Figure A-2. Effect of dietary iron deficiency and overload on ZIP14 levels. A) Western blot analysis of ZIP14 and the quantification by densitometry in rat liver. B) Western blot analysis of ZIP14 and the quantification by densitometry in rat pancreas. C) Western blot analysis of ZIP14 and the quantification by densitometry in rat heart. To indicate lane loading, the blot was stripped and reprobed with the integral membrane protein SR-B1.

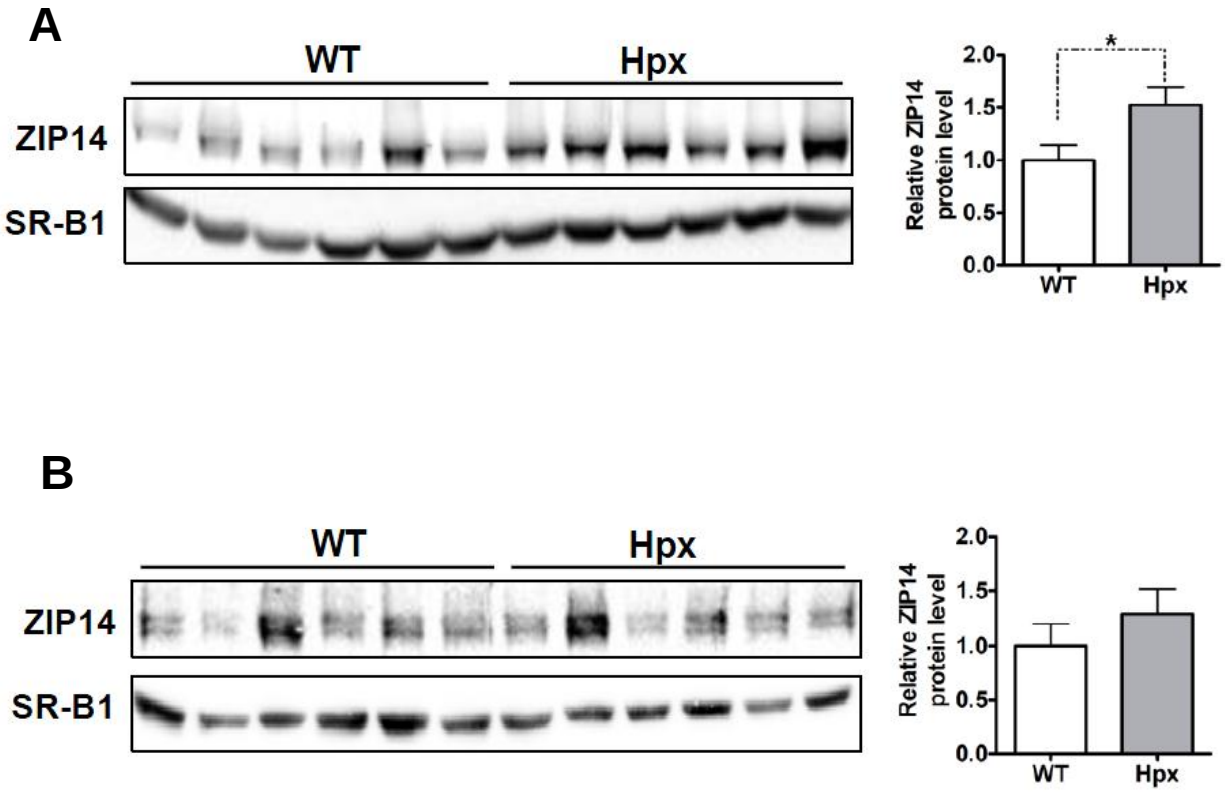

Figure A-3. Effect of genetic iron overload on ZIP14 levels in mouse liver and pancreas. A) Western blot analysis of ZIP14 and the quantification by densitometry in mouse liver. B) Western blot analysis of ZIP14 and the quantification by densitometry in mouse pancreas. To indicate lane loading, the blot was stripped and reprobed with the integral membrane protein SR-B1.

LIST OF REFERENCES

1. Scholander PF. Oxygen transport through hemoglobin solutions. Science 1960;131:585-590.

2. Wittenberg JB. The molecular mechanism of hemoglobin-facilitated oxygen diffusion. J Biol Chem 1966;241:104-114.

3. Wyman J. Facilitated diffusion and the possible role of myoglobin as a transport mechanism. J Biol Chem 1966;241:115-121.

4. Wittenberg JB. Myoglobin-facilitated oxygen diffusion: role of myoglobin in oxygen entry into muscle. Physiol Rev 1970;50:559-636.

5. Chelikani P, Fita I, Loewen PC. Diversity of structures and properties among catalases. Cell Mol Life Sci 2004;61:192-208.

6. Belevich I, Verkhovsky MI, Wikstrom M. Proton-coupled electron transfer drives the proton pump of cytochrome c oxidase. Nature 2006;440:829-832.

7. Hall DO, Evans MC. Iron-sulphur proteins. Nature 1969;223:1342-1348.

8. Beinert H, Kennedy MC. Aconitase, a two-faced protein: enzyme and iron regulatory factor. FASEB J 1993;7:1442-1449.

9. Tuderman L, Myllyla R, Kivirikko KI. Mechanism of the prolyl hydroxylase reaction. 1. Role of co-substrates. Eur J Biochem 1977;80:341-348.

10. Nagatsu T, Levitt M, Udenfriend S. Tyrosine Hydroxylase. The Initial Step in Norepinephrine Biosynthesis. J Biol Chem 1964;239:2910-2917.

11. Smith, Rs. Iron Deficiency and Iron Overload. Arch Dis Child 1965;40:343-363.

12. Andrews NC. Iron homeostasis: insights from genetics and animal models. Nat Rev Genet 2000;1:208-217.

13. Andrews NC. Disorders of iron metabolism. N Engl J Med 1999;341:1986-1995.

14. Munoz M, Villar I, Garcia-Erce JA. An update on iron physiology. World J Gastroenterol 2009;15:4617-4626.

15. Chevion M. A site-specific mechanism for free radical induced biological damage: the essential role of redox-active transition metals. Free Radic Biol Med 1988;5:27-37.

16. Cook JD. Determinants of Non-Heme Iron-Absorption in Man. Food Technology 1983;37:124-126.

17. Carpenter CE, Mahoney AW. Contributions of heme and nonheme iron to human nutrition. Crit Rev Food Sci Nutr 1992;31:333-367.

18. Turnbull A, Cleton F, Finch CA. Iron absorption. IV. The absorption of hemoglobin iron. J Clin Invest 1962;41:1897-1907.

19. Weintraub LR, Weinstein MB, Huser HJ, Rafal S. Absorption of hemoglobin iron: the role of a heme-splitting substance in the intestinal mucosa. J Clin Invest 1968;47:531-539.

20. Parmley RT, Barton JC, Conrad ME, Austin RL, Holland RM. Ultrastructural cytochemistry and radioautography of hemoglobin--iron absorption. Exp Mol Pathol 1981;34:131-144.

21. Donovan A, Brownlie A, Zhou Y, Shepard J, Pratt SJ, Moynihan J, Paw BH, et al. Positional cloning of zebrafish ferroportin1 identifies a conserved vertebrate iron exporter. Nature 2000;403:776-781.

22. McKie AT, Marciani P, Rolfs A, Brennan K, Wehr K, Barrow D, Miret S, et al. A novel duodenal iron-regulated transporter, IREG1, implicated in the basolateral transfer of iron to the circulation. Mol Cell 2000;5:299-309.

23. Shayeghi M, Latunde-Dada GO, Oakhill JS, Laftah AH, Takeuchi K, Halliday N, Khan Y, et al. Identification of an intestinal heme transporter. Cell 2005;122:789-801.

24. Qiu A, Jansen M, Sakaris A, Min SH, Chattopadhyay S, Tsai E, Sandoval C, et al. Identification of an intestinal folate transporter and the molecular basis for hereditary folate malabsorption. Cell 2006;127:917-928.

25. Gunshin H, Mackenzie B, Berger UV, Gunshin Y, Romero MF, Boron WF, Nussberger S, et al. Cloning and characterization of a mammalian proton-coupled metal-ion transporter. Nature 1997;388:482-488.

26. Gunshin H, Fujiwara Y, Custodio AO, Direnzo C, Robine S, Andrews NC. Slc11a2 is required for intestinal iron absorption and erythropoiesis but dispensable in placenta and liver. J Clin Invest 2005;115:1258-1266.

27. Raja KB, Simpson RJ, Peters TJ. Investigation of a role for reduction in ferric iron uptake by mouse duodenum. Biochim Biophys Acta 1992;1135:141-146.

28. Riedel HD, Remus AJ, Fitscher BA, Stremmel W. Characterization and partial purification of a ferrireductase from human duodenal microvillus membranes. Biochem J 1995;309 (Pt 3):745-748.

29. Han O, Failla ML, Hill AD, Morris ER, Smith JC, Jr. Reduction of Fe(III) is required for uptake of nonheme iron by Caco-2 cells. J Nutr 1995;125:1291-1299.

30. Gunshin H, Starr CN, Direnzo C, Fleming MD, Jin J, Greer EL, Sellers VM, et al. Cybrd1 (duodenal cytochrome b) is not necessary for dietary iron absorption in mice. Blood 2005;106:2879-2883.

31. Maeda N, Hagihara H, Nakata Y, Hiller S, Wilder J, Reddick R. Aortic wall damage in mice unable to synthesize ascorbic acid. Proc Natl Acad Sci U S A 2000;97:841-846.

32. Iwama M, Amano A, Shimokado K, Maruyama N, Ishigami A. Ascorbic Acid Levels in Various Tissues, Plasma and Urine of Mice during Aging. J Nutr Sci Vitaminol (Tokyo) 2012;58:169-174.

33. Kim H, Bae S, Yu Y, Kim Y, Kim HR, Hwang YI, Kang JS, et al. The analysis of vitamin C concentration in organs of gulo(-/-) mice upon vitamin C withdrawal. Immune Netw 2012;12:18-26.

34. Vulpe CD, Kuo YM, Murphy TL, Cowley L, Askwith C, Libina N, Gitschier J, et al. Hephaestin, a ceruloplasmin homologue implicated in intestinal iron transport, is defective in the sla mouse. Nat Genet 1999;21:195-199.

35. Grootveld M, Bell JD, Halliwell B, Aruoma OI, Bomford A, Sadler PJ. Non-transferrin-bound iron in plasma or serum from patients with idiopathic hemochromatosis. Characterization by high performance liquid chromatography and nuclear magnetic resonance spectroscopy. J Biol Chem 1989;264:4417-4422.

36. Lovstad RA. Interaction of serum albumin with the Fe(III)-citrate complex. Int J Biochem 1993;25:1015-1017.

37. Breuer W, Hershko C, Cabantchik ZI. The importance of non-transferrin bound iron in disorders of iron metabolism. Transfus Sci 2000;23:185-192.

38. Harrison PM, Arosio P. The ferritins: molecular properties, iron storage function and cellular regulation. Biochim Biophys Acta 1996;1275:161-203.

39. Cohen LA, Gutierrez L, Weiss A, Leichtmann-Bardoogo Y, Zhang DL, Crooks DR, Sougrat R, et al. Serum ferritin is derived primarily from macrophages through a nonclassical secretory pathway. Blood 2010;116:1574-1584.

40. Viprakasit V, Gattermann N, Lee JW, Porter JB, Taher AT, Habr D, Martin N, et al. Geographical variations in current clinical practice on transfusions and iron chelation therapy across various transfusion-dependent anaemias. Blood Transfus 2012:1-14.

41. Ward RJ, Ramsey M, Dickson DP, Hunt C, Douglas T, Mann S, Aquad F, et al. Further characterisation of forms of haemosiderin in iron-overloaded tissues. Eur J Biochem 1994;225:187-194.

42. Ward RJ, Legssyer R, Henry C, Crichton RR. Does the haemosiderin iron core determine its potential for chelation and the development of iron-induced tissue damage? J Inorg Biochem 2000;79:311-317.

43. Ganz T. Hepcidin, a key regulator of iron metabolism and mediator of anemia of inflammation. Blood 2003;102:783-788.

44. Nemeth E. Targeting the hepcidin-ferroportin axis in the diagnosis and treatment of anemias. Adv Hematol 2010;2010:750643.

45. Nemeth E, Tuttle MS, Powelson J, Vaughn MB, Donovan A, Ward DM, Ganz T, et al. Hepcidin regulates cellular iron efflux by binding to ferroportin and inducing its internalization. Science 2004;306:2090-2093.

46. Nicolas G, Chauvet C, Viatte L, Danan JL, Bigard X, Devaux I, Beaumont C, et al. The gene encoding the iron regulatory peptide hepcidin is regulated by anemia, hypoxia, and inflammation. J Clin Invest 2002;110:1037-1044.

47. Pigeon C, Ilyin G, Courselaud B, Leroyer P, Turlin B, Brissot P, Loreal O. A new mouse liver-specific gene, encoding a protein homologous to human antimicrobial peptide hepcidin, is overexpressed during iron overload. J Biol Chem 2001;276:7811-7819.

48. Andersen RV, Tybjaerg-Hansen A, Appleyard M, Birgens H, Nordestgaard BG. Hemochromatosis mutations in the general population: iron overload progression rate. Blood 2004;103:2914-2919.

49. Okada S. Iron-induced tissue damage and cancer: the role of reactive oxygen species-free radicals. Pathol Int 1996;46:311-332.

50. Pietrangelo A. Hereditary hemochromatosis. Annu Rev Nutr 2006;26:251-270.

51. Feder JN, Gnirke A, Thomas W, Tsuchihashi Z, Ruddy DA, Basava A, Dormishian F, et al. A novel MHC class I-like gene is mutated in patients with hereditary haemochromatosis. Nat Genet 1996;13:399-408.

52. Adams PC, Reboussin DM, Barton JC, McLaren CE, Eckfeldt JH, McLaren GD, Dawkins FW, et al. Hemochromatosis and iron-overload screening in a racially diverse population. N Engl J Med 2005;352:1769-1778.

53. Allen KJ, Gurrin LC, Constantine CC, Osborne NJ, Delatycki MB, Nicoll AJ, McLaren CE, et al. Iron-overload-related disease in HFE hereditary hemochromatosis. N Engl J Med 2008;358:221-230.

54. Steinberg KK, Cogswell ME, Chang JC, Caudill SP, McQuillan GM, Bowman BA, Grummer-Strawn LM, et al. Prevalence of C282Y and H63D mutations in the hemochromatosis (HFE) gene in the United States. JAMA 2001;285:2216-2222.

55. Beutler E. The significance of the 187G (H63D) mutation in hemochromatosis. Am J Hum Genet 1997;61:762-764.

56. Burt MJ, George PM, Upton JD, Collett JA, Frampton CM, Chapman TM, Walmsley TA, et al. The significance of haemochromatosis gene mutations in the general population: implications for screening. Gut 1998;43:830-836.

57. Aguilar-Martinez P, Bismuth M, Picot MC, Thelcide C, Pageaux GP, Blanc F, Blanc P, et al. Variable phenotypic presentation of iron overload in H63D homozygotes: are genetic modifiers the cause? Gut 2001;48:836-842.

58. Camaschella C, Roetto A, Cicilano M, Pasquero P, Bosio S, Gubetta L, Di Vito F, et al. Juvenile and adult hemochromatosis are distinct genetic disorders. Eur J Hum Genet 1997;5:371-375.

59. Camaschella C, Roetto A, De Gobbi M. Juvenile hemochromatosis. Semin Hematol 2002;39:242-248.

60. Roetto A, Papanikolaou G, Politou M, Alberti F, Girelli D, Christakis J, Loukopoulos D, et al. Mutant antimicrobial peptide hepcidin is associated with severe juvenile hemochromatosis. Nat Genet 2003;33:21-22.

61. Montosi G, Donovan A, Totaro A, Garuti C, Pignatti E, Cassanelli S, Trenor CC, et al. Autosomal-dominant hemochromatosis is associated with a mutation in the ferroportin (SLC11A3) gene. J Clin Invest 2001;108:619-623.

62. Mayr R, Griffiths WJ, Hermann M, McFarlane I, Halsall DJ, Finkenstedt A, Douds A, et al. Identification of mutations in SLC40A1 that affect ferroportin function and phenotype of human ferroportin iron overload. Gastroenterology 2011;140:2056-2063, 2063 e2051.

63. Njajou OT, Vaessen N, Joosse M, Berghuis B, van Dongen JW, Breuning MH, Snijders PJ, et al. A mutation in SLC11A3 is associated with autosomal dominant hemochromatosis. Nat Genet 2001;28:213-214.

64. Letocart E, Le Gac G, Majore S, Ka C, Radio FC, Gourlaouen I, De Bernardo C, et al. A novel missense mutation in SLC40A1 results in resistance to hepcidin and confirms the existence of two ferroportin-associated iron overload diseases. Br J Haematol 2009;147:379-385.

65. Kushner JP, Porter JP, Olivieri NF. Secondary iron overload. Hematology Am Soc Hematol Educ Program 2001:47-61.

66. Olivieri NF. The beta-thalassemias. N Engl J Med 1999;341:99-109.

67. Cao A, Galanello R. Beta-thalassemia. Genet Med 2010;12:61-76.

68. Brittenham GM. Iron-chelating therapy for transfusional iron overload. N Engl J Med 2011;364:146-156.

69. McLaren GD, Muir WA, Kellermeyer RW. Iron overload disorders: natural history, pathogenesis, diagnosis, and therapy. Crit Rev Clin Lab Sci 1983;19:205-266.

70. Gardenghi S, Grady RW, Rivella S. Anemia, ineffective erythropoiesis, and hepcidin: interacting factors in abnormal iron metabolism leading to iron overload in beta-thalassemia. Hematol Oncol Clin North Am 2010;24:1089-1107.

71. Camaschella C, Piperno A. Hereditary hemochromatosis: recent advances in molecular genetics and clinical management. Haematologica 1997;82:77-84.

72. Neufeld EJ. Oral chelators deferasirox and deferiprone for transfusional iron overload in thalassemia major: new data, new questions. Blood 2006;107:3436-3441.

73. Mackenzie B, Takanaga H, Hubert N, Rolfs A, Hediger MA. Functional properties of multiple isoforms of human divalent metal-ion transporter 1 (DMT1). Biochem J 2007;403:59-69.

74. Lee PL, Gelbart T, West C, Halloran C, Beutler E. The human Nramp2 gene: characterization of the gene structure, alternative splicing, promoter region and polymorphisms. Blood Cells Mol Dis 1998;24:199-215.

75. Hubert N, Hentze MW. Previously uncharacterized isoforms of divalent metal transporter (DMT)-1: implications for regulation and cellular function. Proc Natl Acad Sci U S A 2002;99:12345-12350.

76. Fleming MD, Trenor CC, 3rd, Su MA, Foernzler D, Beier DR, Dietrich WF, Andrews NC. Microcytic anaemia mice have a mutation in Nramp2, a candidate iron transporter gene. Nat Genet 1997;16:383-386.

77. Fleming MD, Romano MA, Su MA, Garrick LM, Garrick MD, Andrews NC. Nramp2 is mutated in the anemic Belgrade (b) rat: evidence of a role for Nramp2 in endosomal iron transport. Proc Natl Acad Sci U S A 1998;95:1148-1153.

78. Su MA, Trenor CC, Fleming JC, Fleming MD, Andrews NC. The G185R mutation disrupts function of the iron transporter Nramp2. Blood 1998;92:2157-2163.

79. Canonne-Hergaux F, Fleming MD, Levy JE, Gauthier S, Ralph T, Picard V, Andrews NC, et al. The Nramp2/DMT1 iron transporter is induced in the duodenum of microcytic anemia mk mice but is not properly targeted to the intestinal brush border. Blood 2000;96:3964-3970.

80. Priwitzerova M, Pospisilova D, Prchal JT, Indrak K, Hlobilkova A, Mihal V, Ponka P, et al. Severe hypochromic microcytic anemia caused by a congenital defect of the iron transport pathway in erythroid cells. Blood 2004;103:3991-3992.

81. Iolascon A, d'Apolito M, Servedio V, Cimmino F, Piga A, Camaschella C. Microcytic anemia and hepatic iron overload in a child with compound heterozygous mutations in DMT1 (SCL11A2). Blood 2006;107:349-354.

82. Beaumont C, Delaunay J, Hetet G, Grandchamp B, de Montalembert M, Tchernia G. Two new human DMT1 gene mutations in a patient with microcytic anemia, low ferritinemia, and liver iron overload. Blood 2006;107:4168-4170.

83. Bardou-Jacquet E, Island ML, Jouanolle AM, Detivaud L, Fatih N, Ropert M, Brissot E, et al. A novel N491S mutation in the human SLC11A2 gene impairs protein trafficking and in association with the G212V mutation leads to microcytic anemia and liver iron overload. Blood Cells Mol Dis 2011;47:243-248.

84. Mims MP, Guan Y, Pospisilova D, Priwitzerova M, Indrak K, Ponka P, Divoky V, et al. Identification of a human mutation of DMT1 in a patient with microcytic anemia and iron overload. Blood 2005;105:1337-1342.

85. Lam-Yuk-Tseung S, Mathieu M, Gros P. Functional characterization of the E399D DMT1/NRAMP2/SLC11A2 protein produced by an exon 12 mutation in a patient with microcytic anemia and iron overload. Blood Cells Mol Dis 2005;35:212-216.

86. Priwitzerova M, Nie G, Sheftel AD, Pospisilova D, Divoky V, Ponka P. Functional consequences of the human DMT1 (SLC11A2) mutation on protein expression and iron uptake. Blood 2005;106:3985-3987.

87. Gunshin H, Jin J, Fujiwara Y, Andrews NC, Mims M, Prchal J. Analysis of the E399D mutation in SLC11A2. Blood 2005;106:2221; author reply 2221-2222.

88. Lam-Yuk-Tseung S, Camaschella C, Iolascon A, Gros P. A novel R416C mutation in human DMT1 (SLC11A2) displays pleiotropic effects on function and causes microcytic anemia and hepatic iron overload. Blood Cells Mol Dis 2006;36:347-354.

89. Blanco E, Kannengiesser C, Grandchamp B, Tasso M, Beaumont C. Not all DMT1 mutations lead to iron overload. Blood Cells Mol Dis 2009;43:199-201.

90. Edwards JA, Hoke JE. Red cell iron uptake in hereditary microcytic anemia. Blood 1975;46:381-388.

91. Edwards JA, Sullivan AL, Hoke JE. Defective delivery of iron to the developing red cell of the Belgrade laboratory rat. Blood 1980;55:645-648.

92. Farcich EA, Morgan EH. Uptake of transferrin-bound and nontransferrin-bound iron by reticulocytes from the Belgrade laboratory rat: comparison with Wistar rat transferrin and reticulocytes. Am J Hematol 1992;39:9-14.

93. Garrick MD, Gniecko K, Liu Y, Cohan DS, Garrick LM. Transferrin and the transferrin cycle in Belgrade rat reticulocytes. J Biol Chem 1993;268:14867-14874.

94. Canonne-Hergaux F, Zhang AS, Ponka P, Gros P. Characterization of the iron transporter DMT1 (NRAMP2/DCT1) in red blood cells of normal and anemic mk/mk mice. Blood 2001;98:3823-3830.

95. Ohgami RS, Campagna DR, Greer EL, Antiochos B, McDonald A, Chen J, Sharp JJ, et al. Identification of a ferrireductase required for efficient transferrin-dependent iron uptake in erythroid cells. Nat Genet 2005;37:1264-1269.

96. Oates PS, Morgan EH. Defective iron uptake by the duodenum of Belgrade rats fed diets of different iron contents. Am J Physiol 1996;270:G826-832.

97. Garrick M, Scott D, Walpole S, Finkelstein E, Whitbred J, Chopra S, Trivikram L, et al. Iron supplementation moderates but does not cure the Belgrade anemia. Biometals 1997;10:65-76.

98. Dupic F, Fruchon S, Bensaid M, Loreal O, Brissot P, Borot N, Roth MP, et al. Duodenal mRNA expression of iron related genes in response to iron loading and iron deficiency in four strains of mice. Gut 2002;51:648-653.

99. Stuart KA, Anderson GJ, Frazer DM, Powell LW, McCullen M, Fletcher LM, Crawford DH. Duodenal expression of iron transport molecules in untreated haemochromatosis subjects. Gut 2003;52:953-959.

100. Kong WN, Chang YZ, Wang SM, Zhai XL, Shang JX, Li LX, Duan XL. Effect of erythropoietin on hepcidin, DMT1 with IRE, and hephaestin gene expression in duodenum of rats. J Gastroenterol 2008;43:136-143.

101. Kelleher T, Ryan E, Barrett S, Sweeney M, Byrnes V, O'Keane C, Crowe J. Increased DMT1 but not IREG1 or HFE mRNA following iron depletion therapy in hereditary haemochromatosis. Gut 2004;53:1174-1179.

102. Canonne-Hergaux F, Levy JE, Fleming MD, Montross LK, Andrews NC, Gros P. Expression of the DMT1 (NRAMP2/DCT1) iron transporter in mice with genetic iron overload disorders. Blood 2001;97:1138-1140.

103. Chen H, Su T, Attieh ZK, Fox TC, McKie AT, Anderson GJ, Vulpe CD. Systemic regulation of Hephaestin and Ireg1 revealed in studies of genetic and nutritional iron deficiency. Blood 2003;102:1893-1899.

104. Nicolas G, Bennoun M, Devaux I, Beaumont C, Grandchamp B, Kahn A, Vaulont S. Lack of hepcidin gene expression and severe tissue iron overload in upstream stimulatory factor 2 (USF2) knockout mice. Proc Natl Acad Sci U S A 2001;98:8780-8785.

105. Viatte L, Lesbordes-Brion JC, Lou DQ, Bennoun M, Nicolas G, Kahn A, Canonne-Hergaux F, et al. Deregulation of proteins involved in iron metabolism in hepcidin-deficient mice. Blood 2005;105:4861-4864.

106. Chung B, Chaston T, Marks J, Srai SK, Sharp PA. Hepcidin decreases iron transporter expression in vivo in mouse duodenum and spleen and in vitro in THP-1 macrophages and intestinal Caco-2 cells. J Nutr 2009;139:1457-1462.

107. Fleming RE, Migas MC, Zhou X, Jiang J, Britton RS, Brunt EM, Tomatsu S, et al. Mechanism of increased iron absorption in murine model of hereditary hemochromatosis: increased duodenal expression of the iron transporter DMT1. Proc Natl Acad Sci U S A 1999;96:3143-3148.

108. Kawabata H, Fleming RE, Gui D, Moon SY, Saitoh T, O'Kelly J, Umehara Y, et al. Expression of hepcidin is down-regulated in TfR2 mutant mice manifesting a phenotype of hereditary hemochromatosis. Blood 2005;105:376-381.

109. Wang RH, Li C, Xu X, Zheng Y, Xiao C, Zerfas P, Cooperman S, et al. A role of SMAD4 in iron metabolism through the positive regulation of hepcidin expression. Cell Metab 2005;2:399-409.

110. Ahmad KA, Ahmann JR, Migas MC, Waheed A, Britton RS, Bacon BR, Sly WS, et al. Decreased liver hepcidin expression in the Hfe knockout mouse. Blood Cells Mol Dis 2002;29:361-366.

111. Bridle KR, Frazer DM, Wilkins SJ, Dixon JL, Purdie DM, Crawford DH, Subramaniam VN, et al. Disrupted hepcidin regulation in HFE-associated haemochromatosis and the liver as a regulator of body iron homoeostasis. Lancet 2003;361:669-673.

112. Nemeth E, Roetto A, Garozzo G, Ganz T, Camaschella C. Hepcidin is decreased in TFR2 hemochromatosis. Blood 2005;105:1803-1806.

113. Zoller H, Koch RO, Theurl I, Obrist P, Pietrangelo A, Montosi G, Haile DJ, et al. Expression of the duodenal iron transporters divalent-metal transporter 1 and ferroportin 1 in iron deficiency and iron overload. Gastroenterology 2001;120:1412-1419.

114. Rolfs A, Bonkovsky HL, Kohlroser JG, McNeal K, Sharma A, Berger UV, Hediger MA. Intestinal expression of genes involved in iron absorption in humans. Am J Physiol Gastrointest Liver Physiol 2002;282:G598-607.

115. Casey JL, Hentze MW, Koeller DM, Caughman SW, Rouault TA, Klausner RD, Harford JB. Iron-responsive elements: regulatory RNA sequences that control mRNA levels and translation. Science 1988;240:924-928.

116. Koeller DM, Casey JL, Hentze MW, Gerhardt EM, Chan LN, Klausner RD, Harford JB. A cytosolic protein binds to structural elements within the iron regulatory region of the transferrin receptor mRNA. Proc Natl Acad Sci U S A 1989;86:3574-3578.

117. Casey JL, Koeller DM, Ramin VC, Klausner RD, Harford JB. Iron regulation of transferrin receptor mRNA levels requires iron-responsive elements and a rapid turnover determinant in the 3' untranslated region of the mRNA. EMBO J 1989;8:3693-3699.

118. Gunshin H, Allerson CR, Polycarpou-Schwarz M, Rofts A, Rogers JT, Kishi F, Hentze MW, et al. Iron-dependent regulation of the divalent metal ion transporter. FEBS Lett 2001;509:309-316.

119. Galy B, Ferring-Appel D, Kaden S, Grone HJ, Hentze MW. Iron regulatory proteins are essential for intestinal function and control key iron absorption molecules in the duodenum. Cell Metab 2008;7:79-85.

120. Smith TG, Robbins PA, Ratcliffe PJ. The human side of hypoxia-inducible factor. Br J Haematol 2008;141:325-334.

121. Mastrogiannaki M, Matak P, Keith B, Simon MC, Vaulont S, Peyssonnaux C. HIF-2alpha, but not HIF-1alpha, promotes iron absorption in mice. J Clin Invest 2009;119:1159-1166.

122. Vanoaica L, Darshan D, Richman L, Schumann K, Kuhn LC. Intestinal ferritin H is required for an accurate control of iron absorption. Cell Metab 2010;12:273-282.

123. Trinder D, Oates PS, Thomas C, Sadleir J, Morgan EH. Localisation of divalent metal transporter 1 (DMT1) to the microvillus membrane of rat duodenal enterocytes in iron deficiency, but to hepatocytes in iron overload. Gut 2000;46:270-276.

124. Kim DW, Kim KY, Choi BS, Youn P, Ryu DY, Klaassen CD, Park JD. Regulation of metal transporters by dietary iron, and the relationship between body iron levels and cadmium uptake. Arch Toxicol 2007;81:327-334.

125. Muckenthaler M, Roy CN, Custodio AO, Minana B, deGraaf J, Montross LK, Andrews NC, et al. Regulatory defects in liver and intestine implicate abnormal hepcidin and Cybrd1 expression in mouse hemochromatosis. Nat Genet 2003;34:102-107.

126. Chua AC, Olynyk JK, Leedman PJ, Trinder D. Nontransferrin-bound iron uptake by hepatocytes is increased in the Hfe knockout mouse model of hereditary hemochromatosis. Blood 2004;104:1519-1525.

127. Foot NJ, Dalton HE, Shearwin-Whyatt LM, Dorstyn L, Tan SS, Yang B, Kumar S. Regulation of the divalent metal ion transporter DMT1 and iron homeostasis by a ubiquitin-dependent mechanism involving Ndfips and WWP2. Blood 2008;112:4268-4275.

128. Howitt J, Putz U, Lackovic J, Doan A, Dorstyn L, Cheng H, Yang B, et al. Divalent metal transporter 1 (DMT1) regulation by Ndfip1 prevents metal toxicity in human neurons. Proc Natl Acad Sci U S A 2009;106:15489-15494.

129. Foot NJ, Leong YA, Dorstyn LE, Dalton HE, Ho K, Zhao L, Garrick MD, et al. Ndfip1-deficient mice have impaired DMT1 regulation and iron homeostasis. Blood 2011;117:638-646.

130. Jenkitkasemwong S, Wang CY, Mackenzie B, Knutson MD. Physiologic implications of metal-ion transport by ZIP14 and ZIP8. Biometals 2012.

131. Eide DJ. The SLC39 family of metal ion transporters. Pflugers Arch 2004;447:796-800.

132. Eng BH, Guerinot ML, Eide D, Saier MH, Jr. Sequence analyses and phylogenetic characterization of the ZIP family of metal ion transport proteins. J Membr Biol 1998;166:1-7.

133. Taylor KM, Morgan HE, Johnson A, Nicholson RI. Structure-function analysis of a novel member of the LIV-1 subfamily of zinc transporters, ZIP14. FEBS Lett 2005;579:427-432.

134. Tominaga K, Kagata T, Johmura Y, Hishida T, Nishizuka M, Imagawa M. SLC39A14, a LZT protein, is induced in adipogenesis and transports zinc. FEBS J 2005;272:1590-1599.

135. Liuzzi JP, Aydemir F, Nam H, Knutson MD, Cousins RJ. Zip14 (Slc39a14) mediates non-transferrin-bound iron uptake into cells. Proc Natl Acad Sci U S A 2006;103:13612-13617.

136. Pinilla-Tenas JJ, Sparkman BK, Shawki A, Illing AC, Mitchell CJ, Zhao N, Liuzzi JP, et al. Zip14 is a complex broad-scope metal-ion transporter whose functional properties support roles in the cellular uptake of zinc and nontransferrin-bound iron. Am J Physiol Cell Physiol 2011;301:C862-871.

137. Zhao N, Gao J, Enns CA, Knutson MD. ZRT/IRT-like protein 14 (ZIP14) promotes the cellular assimilation of iron from transferrin. J Biol Chem 2010;285:32141-32150.

138. Begum NA, Kobayashi M, Moriwaki Y, Matsumoto M, Toyoshima K, Seya T. Mycobacterium bovis BCG cell wall and lipopolysaccharide induce a novel gene, BIGM103, encoding a 7-TM protein: identification of a new protein family having Zn-transporter and Zn-metalloprotease signatures. Genomics 2002;80:630-645.

139. Dalton TP, He L, Wang B, Miller ML, Jin L, Stringer KF, Chang X, et al. Identification of mouse SLC39A8 as the transporter responsible for cadmium-induced toxicity in the testis. Proc Natl Acad Sci U S A 2005;102:3401-3406.

140. He L, Girijashanker K, Dalton TP, Reed J, Li H, Soleimani M, Nebert DW. ZIP8, member of the solute-carrier-39 (SLC39) metal-transporter family: characterization of transporter properties. Mol Pharmacol 2006;70:171-180.

141. Nam H, Knutson MD. Effect of dietary iron deficiency and overload on the expression of ZIP metal-ion transporters in rat liver. Biometals 2012;25:115-124.

142. Collins JF, Franck CA, Kowdley KV, Ghishan FK. Identification of differentially expressed genes in response to dietary iron deprivation in rat duodenum. Am J Physiol Gastrointest Liver Physiol 2005;288:G964-971.

143. Liuzzi JP, Lichten LA, Rivera S, Blanchard RK, Aydemir TB, Knutson MD, Ganz T, et al. Interleukin-6 regulates the zinc transporter Zip14 in liver and contributes to the hypozincemia of the acute-phase response. Proc Natl Acad Sci U S A 2005;102:6843-6848.

144. Thambiayya K, Wasserloos KJ, Huang Z, Kagan VE, St Croix CM, Pitt BR. LPS-induced decrease in intracellular labile zinc, [Zn]i, contributes to apoptosis in cultured sheep pulmonary artery endothelial cells. Am J Physiol Lung Cell Mol Physiol 2011;300:L624-632.

145. Aydemir TB, Liuzzi JP, McClellan S, Cousins RJ. Zinc transporter ZIP8 (SLC39A8) and zinc influence IFN-gamma expression in activated human T cells. J Leukoc Biol 2009;86:337-348.

146. Wang B, Schneider SN, Dragin N, Girijashanker K, Dalton TP, He L, Miller ML, et al. Enhanced cadmium-induced testicular necrosis and renal proximal tubule damage caused by gene-dose increase in a Slc39a8-transgenic mouse line. Am J Physiol Cell Physiol 2007;292:C1523-1535.

147. Girijashanker K, He L, Soleimani M, Reed JM, Li H, Liu Z, Wang B, et al. Slc39a14 gene encodes ZIP14, a metal/bicarbonate symporter: similarities to the ZIP8 transporter. Mol Pharmacol 2008;73:1413-1423.

148. Besecker B, Bao S, Bohacova B, Papp A, Sadee W, Knoell DL. The human zinc transporter SLC39A8 (Zip8) is critical in zinc-mediated cytoprotection in lung epithelia. Am J Physiol Lung Cell Mol Physiol 2008;294:L1127-1136.

149. Liu Z, Li H, Soleimani M, Girijashanker K, Reed JM, He L, Dalton TP, et al. Cd2+ versus Zn2+ uptake by the ZIP8 HCO3--dependent symporter: kinetics, electrogenicity and trafficking. Biochem Biophys Res Commun 2008;365:814-820.

150. Speliotes EK, Willer CJ, Berndt SI, Monda KL, Thorleifsson G, Jackson AU, Lango Allen H, et al. Association analyses of 249,796 individuals reveal 18 new loci associated with body mass index. Nat Genet 2010;42:937-948.

151. Waterworth DM, Ricketts SL, Song K, Chen L, Zhao JH, Ripatti S, Aulchenko YS, et al. Genetic variants influencing circulating lipid levels and risk of coronary artery disease. Arterioscler Thromb Vasc Biol 2010;30:2264-2276.

152. Carrera N, Arrojo M, Sanjuan J, Ramos-Rios R, Paz E, Suarez-Rama JJ, Paramo M, et al. Association study of nonsynonymous single nucleotide polymorphisms in schizophrenia. Biol Psychiatry 2012;71:169-177.

153. Raymond AD, Gekonge B, Giri MS, Hancock A, Papasavvas E, Chehimi J, Kossenkov AV, et al. Increased metallothionein gene expression, zinc, and zinc-dependent resistance to apoptosis in circulating monocytes during HIV viremia. J Leukoc Biol 2010;88:589-596.

154. Besecker BY, Exline MC, Hollyfield J, Phillips G, Disilvestro RA, Wewers MD, Knoell DL. A comparison of zinc metabolism, inflammation, and disease severity in critically ill infected and noninfected adults early after intensive care unit admission. Am J Clin Nutr 2011;93:1356-1364.

155. Levy JE, Montross LK, Cohen DE, Fleming MD, Andrews NC. The C282Y mutation causing hereditary hemochromatosis does not produce a null allele. Blood 1999;94:9-11.

156. Trenor CC, 3rd, Campagna DR, Sellers VM, Andrews NC, Fleming MD. The molecular defect in hypotransferrinemic mice. Blood 2000;96:1113-1118.

157. Knutson MD, Walter PB, Ames BN, Viteri FE. Both iron deficiency and daily iron supplements increase lipid peroxidation in rats. J Nutr 2000;130:621-628.

158. Worthington MT, Browne L, Battle EH, Luo RQ. Functional properties of transfected human DMT1 iron transporter. Am J Physiol Gastrointest Liver Physiol 2000;279:G1265-1273.

159. Batey RG, Shamir S, Wilms J. Properties and hepatic metabolism of non-transferrin-bound iron. Dig Dis Sci 1981;26:1084-1088.

160. Scheiber-Mojdehkar B, Zimmermann I, Dresow B, Goldenberg H. Differential response of non-transferrin bound iron uptake in rat liver cells on long-term and short-term treatment with iron. J Hepatol 1999;31:61-70.

161. Shindo M, Torimoto Y, Saito H, Motomura W, Ikuta K, Sato K, Fujimoto Y, et al. Functional role of DMT1 in transferrin-independent iron uptake by human hepatocyte and hepatocellular carcinoma cell, HLF. Hepatol Res 2006;35:152-162.

162. Thompson K, Molina RM, Brain JD, Wessling-Resnick M. Belgrade rats display liver iron loading. J Nutr 2006;136:3010-3014.

163. Graham RM, Chua AC, Herbison CE, Olynyk JK, Trinder D. Liver iron transport. World J Gastroenterol 2007;13:4725-4736.

164. Bergmann OM, Mathahs MM, Broadhurst KA, Weydert JA, Wilkinson N, Howe JR, Han O, et al. Altered expression of iron regulatory genes in cirrhotic human livers: clues to the cause of hemosiderosis? Lab Invest 2008;88:1349-1357.

165. Anderson GJ, Vulpe CD. Mammalian iron transport. Cell Mol Life Sci 2009;66:3241-3261.

166. Chepelev NL, Willmore WG. Regulation of iron pathways in response to hypoxia. Free Radic Biol Med 2011;50:645-666.

167. Takami T, Sakaida I. Iron regulation by hepatocytes and free radicals. J Clin Biochem Nutr 2011;48:103-106.

168. Brissot P, Ropert M, Le Lan C, Loreal O. Non-transferrin bound iron: A key role in iron overload and iron toxicity. Biochim Biophys Acta 2012;1820:403-410.

169. Li YQ, Bai B, Cao XX, Zhang YH, Yan H, Zheng QQ, Zhuang GH. Divalent metal transporter 1 expression and regulation in human placenta. Biol Trace Elem Res 2012;146:6-12.

170. Yamasaki T, Sakaida I. Hepatic arterial infusion chemotherapy for advanced hepatocellular carcinoma and future treatments for the poor responders. Hepatol Res 2012;42:340-348.

171. Zhou XY, Tomatsu S, Fleming RE, Parkkila S, Waheed A, Jiang J, Fei Y, et al. HFE gene knockout produces mouse model of hereditary hemochromatosis. Proc Natl Acad Sci U S A 1998;95:2492-2497.

172. Craven CM, Alexander J, Eldridge M, Kushner JP, Bernstein S, Kaplan J. Tissue distribution and clearance kinetics of non-transferrin-bound iron in the hypotransferrinemic mouse: a rodent model for hemochromatosis. Proc Natl Acad Sci U S A 1987;84:3457-3461.

173. Postic C, Shiota M, Niswender KD, Jetton TL, Chen Y, Moates JM, Shelton KD, et al. Dual roles for glucokinase in glucose homeostasis as determined by liver and pancreatic beta cell-specific gene knock-outs using Cre recombinase. J Biol Chem 1999;274:305-315.

174. Bradbury MW, Raja K, Ueda F. Contrasting uptakes of 59Fe into spleen, liver, kidney and some other soft tissues in normal and hypotransferrinaemic mice. Influence of an antibody against the transferrin receptor. Biochem Pharmacol 1994;47:969-974.

175. Wang CY, Jenkitkasemwong S, Sparkman BK, Shawki A, Mackenzie B, Knutson MD. Metal transport, subcellular localization, and tissue distribution of Zip8, a Zip14 homologue. FASEB J. 2012;26.

176. Galvez-Peralta M, He L, Jorge-Nebert LF, Wang B, Miller ML, Eppert BL, Afton S, et al. ZIP8 Zinc Transporter: Indispensable Role for Both Multiple-Organ Organogenesis and Hematopoiesis In Utero. PLoS One 2012;7:e36055.

177. Wang CY, Jenkitkasemwong S, Duarte S, Sparkman B, Shawki A, Mackenzie B, Knutson MD. ZIP8 Is an Iron and Zinc Transporter Whose Cell-surface Expression Is Upregulated by Cellular Iron Loading. J Biol Chem 2012.

178. Morgan EH, Smith GD, Peters TJ. Uptake and subcellular processing of 59Fe-125I-labelled transferrin by rat liver. Biochem J 1986;237:163-173.

179. Kawabata H, Germain RS, Ikezoe T, Tong X, Green EM, Gombart AF, Koeffler HP. Regulation of expression of murine transferrin receptor 2. Blood 2001;98:1949-1954.

180. Adams PC, Bradley C, Frei JV. Hepatic zinc in hemochromatosis. Clin Invest Med 1991;14:16-20.

181. Vayenas DV, Repanti M, Vassilopoulos A, Papanastasiou DA. Influence of iron overload on manganese, zinc, and copper concentration in rat tissues in vivo: study of liver, spleen, and brain. Int J Clin Lab Res 1998;28:183-186.

182. Anderson GJ, Frazer DM. Hepatic iron metabolism. Semin Liver Dis 2005;25:420-432.

183. Kumfu S, Chattipakorn S, Srichairatanakool S, Settakorn J, Fucharoen S, Chattipakorn N. T-type calcium channel as a portal of iron uptake into cardiomyocytes of beta-thalassemic mice. Eur J Haematol 2011;86:156-166.

184. Hojyo S, Fukada T, Shimoda S, Ohashi W, Bin BH, Koseki H, Hirano T. The Zinc Transporter SLC39A14/ZIP14 Controls G-Protein Coupled Receptor-Mediated Signaling Required for Systemic Growth. PLoS One 2011;6.

185. Hahn P, Song Y, Ying GS, He X, Beard J, Dunaief JL. Age-dependent and gender-specific changes in mouse tissue iron by strain. Exp Gerontol 2009;44:594-600.

BIOGRAPHICAL SKETCH

Chia-Yu Wang was born in Taoyuan, Taiwan. She received her Bachelor of Education degree in Nutritional Science and in Health Education from National Taiwan Normal University, Taipei, Taiwan. She worked with Dr. Li-Ching Lyu as an undergraduate volunteer and helped in database management as well as initial statistical analysis in a prospective study of dietary intakes and influential factors from pregnancy to postpartum on maternal weight retention in Taipei.

In August 2005, she came to the Department of Nutrition for the master's program at University of Massachusetts, Amherst and reapplied for PhD program one year after working with the late Dr. Hiromi Gunshin in molecular mechanisms of liver iron accumulation. She joined Dr. Mitchell Knutson in the Department of Food Science and Human Nutrition for the PhD program in Nutritional Science at University of Florida in August 2008, continued her work in molecular aspects of iron metabolism.